



โครงการการเรียนการสอนเพื่อเสริมประสบการณ์

ระบบรอยแตกธรรมชาติในกลุ่มหินโคราช
อำเภอเทพสถิต จังหวัดชัยภูมิ

โดย

นายคณิตพงศ์ เอี่ยมสินธร

เลขประจำตัวนิต 5732706823

โครงการนี้เป็นส่วนหนึ่งของการศึกษาระดับปริญญาตรี
ภาควิชาธรณีวิทยา คณะวิทยาศาสตร์ จุฬาลงกรณ์มหาวิทยาลัย

ปีการศึกษา 2560

บทคัดย่อและแฟ้มข้อมูลฉบับเต็มของโครงการทางวิชาการที่ให้บริการในคลังปัญญาจุฬาฯ (CUIR)

เป็นแฟ้มข้อมูลของนิสิตเจ้าของโครงการทางวิชาการที่ส่งผ่านทางคณะที่สังกัด

The abstract and full text of senior projects in Chulalongkorn University Intellectual Repository (CUIR)

are the senior project authors' files submitted through the faculty.

NATURAL FRACTURE SYSTEM IN KHORAT GROUP,
THEP SATHIT DISTRICT, CHAIYAPHUM PROVINCE

Mr.Khanitpong Aiemsintorn

A Project Submitted in Partial Fulfillment of the Requirements
for the Degree of Bachelor of Science Program in Geology
Department of Geology, Faculty of Science, Chulalongkorn University
Academic Year 2017

ระบบรอยแตกธรรมชาติในกลุ่มหินโคราช อำเภอเทพสถิต จังหวัดชัยภูมิ

นายคณิตพงศ์ เอี่ยมสินธร

โครงการนี้เป็นส่วนหนึ่งของการศึกษาตามหลักสูตรวิทยาศาสตรบัณฑิต

ภาควิชาธรณีวิทยา คณะวิทยาศาสตร์ จุฬาลงกรณ์มหาวิทยาลัย

ปีการศึกษา 2560

Project Title	NATURAL FRACTURE SYSTEM IN KHORAT GROUP, THEP SATHIT DISTRICT, CHAIYAPHUM PROVINCE
By	Mr.Khanitpong Aiemsintorn
Field of Study	Geology
Project Advisor	Sukonmeth Jitmahantakul, Ph.D.

Submitted date.....

Approval date.....

.....

Project Advisor

(Sukonmeth Jitmahantakul, Ph.D.)

คณิตพงศ์ เอี่ยมสินธร : ระบบรอยแตกธรรมชาติในกลุ่มหินโคราช อำเภอเทพสถิต จังหวัดชัยภูมิ (NATURAL FRACTURE SYSTEM IN KHORAT GROUP, THEP SATHIT DISTRICT, CHAIYAPHUM PROVINCE) อ.ที่ปรึกษาโครงการหลัก : ดร.สุคนธ์เมธ จิตรมหันตกุล, 42 หน้า.

บริเวณผ่าสุดแผ่นดินซึ่งเป็นแหล่งท่องเที่ยวของอำเภอเทพสถิต จังหวัดชัยภูมิ มีลักษณะเด่นของแหล่งท่องเที่ยวอยู่สองประการคือการยกตัวเป็นหน้าผาสูงชัน และมีรอยแตกที่เกิดขึ้นอย่างเป็นระบบ โดยการยกตัวเป็นหน้าผาสูงได้มีการทำป้ายอธิบายการเกิดด้วยกระบวนการทางธรณีวิทยาไว้แล้วแต่ข้อมูลในป้ายยังไม่สอดคล้องกับความรู้ทางธรณีวิทยาในปัจจุบัน ส่วนระบบรอยแตกยังไม่มีการอธิบายใดๆว่ารอยแตกนั้นเกิดขึ้นมาได้อย่างไรมีความสัมพันธ์กับแรงในทิศทางใด และเมื่อสังเกตจากแบบจำลองความสูงเชิงเลขจะพบโครงสร้างเชิงเส้นกระจายตัวอยู่ทั่วบริเวณขอบด้านตะวันตกของอำเภอเทพสถิต การศึกษาครั้งนี้ทำเพื่อจัดทำแผนที่รอยแตกของกลุ่มหินโคราชบริเวณขอบตะวันตกของที่ราบสูงโคราชและเพื่อเสนอสมมติฐานแบบจำลองการเกิดรอยแตกบริเวณขอบตะวันตกของที่ราบสูงโคราชโดยใช้ข้อมูลรอยแตกจากการศึกษาในภาคสนามและการแปลแนวแตกจากแบบจำลองหินโผล่ดิจิทัล (Digital outcrop model; DOM) และแบบจำลองความสูงเชิงเลข (Digital elevation model; DEM) จากการศึกษาครั้งนี้พบว่าบริเวณขอบทางด้านตะวันตกของที่ราบสูงโคราชประกอบไปด้วยรอยแตก 3 แนว ได้แก่ แนวตะวันออกเฉียงเหนือ-ตะวันตกเฉียงใต้เป็นรอยแตกที่มีการเลื่อนตัวตามระนาบรอยแตกแบบซ้ายเข้า แนวตะวันตกเฉียงเหนือ-ตะวันออกเฉียงใต้เป็นรอยแตกที่มีการเลื่อนตัวตามระนาบรอยแตกแบบขวาเข้า และแนวแตกในแนวเหนือ-ใต้เป็นรอยแตกแบบเปิดออกมีการเลื่อนตัวในทิศทางตั้งฉากกับระนาบรอยแตก จากทิศทางการวางตัวและชนิดของรอยแตกบ่งบอกว่ารอยแตกเหล่านี้เกิดจากความเค้นอัดพื้นฐานที่มากที่สุดที่ในแนวเหนือ-ใต้ ความเค้นดังกล่าวนี้เป็นผลจากธรณีแปรสัณฐานการชนกันระหว่างแผ่นเปลือกโลกอินเดียและเอเชียในช่วงยุคพาลีโอจีน นอกจากนั้นแล้วความเค้นดังกล่าวยังทำให้เกิดรอยเลื่อนแบบซ้ายเข้าและการยกตัวของขอบทางด้านตะวันตกของที่ราบสูงโคราชบริเวณอำเภอเทพสถิต

ภาควิชา.....ธรณีวิทยา.....ลายมือชื่อนิสิต.....
 สาขาวิชา.....ธรณีวิทยา.....ลายมือชื่อ อ.ที่ปรึกษาหลัก.....
 ปีการศึกษา.....2560.....

5732706823 : MAJOR GEOLOGY

KEYWORDS : KHORAT GROUP / HIMALAYAN OROGENY / FRACTURE / STRIKE-SLIP FAULT/ KHORAT PLATEAU

KHANITPONG AIEMSINTORN : NATURAL FRACTURE SYSTEM IN KHORAT GROUP, THEP SATHIT DISTRICT, CHAIYAPHUM PROVINCE. ADVISOR : SUKONMETH JITMAHANTAKUL, Ph.D., pp.

Cliff top land or Phasudpandin is tourist attraction in Thep Sathit District, Chaiyaphum Province. There are two remarkable features in Phasudpandin. One is the feature of cliff and the other is systemic fractures scattered throughout the cliff. Geological event, that is a cause of cliff lifting, is described on the board in Phasudpandin. Unfortunately, the content on the board isn't consistent with current geological knowledge and there is no information about systematic fracture. Observed from Digital elevation model, there are a lot of fractures scattered throughout the western boundary of Thep Sathit district, which seem to be related with systematic fractures in Phasudpandin. In this study, field study, digital outcrop model, and digital elevation model were used to create fracture map and propose a conceptual model for fracture development of Khorat Group in western part of Thep Sathit district, Chaiyaphum province. Results from this study show that there are 3 main orientations and types of fracture scattered throughout the area: ENE-WSW (sinistral), WNW-ESE (dextral) and N-S (extension fracture). The orientations and types of fracture imply that these fractures are caused by maximum compressive principle stress in N-S direction which is a result of collision between India plate and Eurasia plate in Paleogene. This compression is also a cause of faulting and uplifting along western margin of Thep Sathit district. The compression direction suggests that fault along western margin of district is sinistral strike-slip fault.

Department :.....Geology.....Student's Signature.....

Field of Study :.....Geology..... Advisor's Signature.....

Academic Year :...2017.....

Acknowledgements

I would like to express my appreciation to my advisor Dr.Sukonmeth Jitmahantakul for his support,suggestions, and valuable ideas during this work. I have learned not only the invaluable vision on research, but also many skills and knowledges that improved me a lot.

I am very grateful to Assoc. Prof. Dr. Pitsanupong Kanjanapayont for his advices and knowledge about structural geology.

I would like to give a special thanks to Poorinut Thipo, Natcharphol Charnsiri for helping me collect field data. It was a great 2 day with my lovely friends.

I have furthermore to thank the entire department of Geology stuff for supporting everything during study here.

Especially, I would like to thank our senior project team, Khanitpong Aiemsintorn, Narudee Saikrasin and Rungkarn Thammasanya and my classmates for their friendship, and encouragement. It has been a great experience knowing all of you.

Finally, my deepest gratitude goes to my family who always stays with me in a good and bad time.

List of Contents

Abstract in Thai	iv
Abstract in English	v
Acknowledgements	vi
List of Contents	vii
List of Figures	viii
Chapter 1 Introduction	1
1.1 Introduction	1
1.2 Study Area	2
Chapter 2 Geological Background	3
2.1 Stratigraphy	3
2.2 Geological setting	6
2.3 Fracture type	6
2.4 Dihedral angle	7
Chapter 3 Methodology	9
3.1 Data collection	9
3.2 Digital outcrop model construction	9
3.3 Fracture analysis	12
3.3.1 Various directional sun azimuth in DOM	12
3.3.2 Mesh selection analysis	12
3.4 Stress Analysis	12
Chapter 4 Results	19
4.1 Fracture orientation	19
4.1.1 Digital elevation model	19
4.1.2 Digital Outcrop	19
4.1.3 Field observation	20
4.2 Fracture classification	27
4.3 Stress analysis	34
Chapter 5 Discussion	35
5.1 Mesh selection analysis and Visual interpretation	35
5.2 E-W fracture trend in DEM	35
5.3 Maximum compressive principle stress direction	35
5.4 Unusual high dihedral angle	35
5.5 Conceptual model for fracture development	36
Chapter 6 Conclusions	40
References	41
Appendix	43

List of Figures

		Page
Figure 1.1	Satellite image showing boundary of Thep sathit district, and location of field observation.	2
Figure 2.1	Geological map of Chaiyaphum province.	4
Figure 2.2	Regional stratigraphy shows Lithology, sequence of rocks, age of rock and key events during Permian to Tertiary. Rocks in study area is in Cretaceous age. The red rectangular frame emphasize two tectonic events after deposition of rock in study area.	5
Figure 2.3	Tectonic evolution of Thailand from Late Palaeozoic to Cainozoic.	7
Figure 2.4	The types of fracture.	8
Figure 3.1	Methodology showing the four main stages of this study.	10
Figure 3.2	Four main procedures of Digital Outcrop Model construction by using Photoscan software.	11
Figure 3.3	Variation of sun azimuth, a) N-S direction, b) NE-SW direction, c) E-S direction and d) SE-NW direction, showing different in fracture intensity.	13
Figure 3.4	Dip attribute showing all various dip angles of mesh in Phasudpandin. The red rectangular frame showing location of figure3.5.	14
Figure 3.5	Showing dip angle on fracture plane (red area) higher than surface plane.(blue area).	15
Figure 3.6	The rest meshes (dip>60°) representing fracture orientation in Phasudpandin.	16

- Figure 3.7** Azimuth of rest mesh showing the different mesh colour in each fracture trend. Purple meshes representing NE-SW fracture trend. Yellow meshes representing NW-SE fracture trend. Showing variation of colour or mesh orientation in one fracture trend. NE-SW has some green meshes and NW-SE has some blue meshes. 17
- Figure 3.8** Relationship of principle stresses, Extension fracture, Shear fracture, maximum principle stress (σ_1), intermediate principle stress (σ_2), minimum principle stress (σ_3) and A : Dihedral angle. 18
- Figure 4.1** Digital elevation model of Thep sathit district. The blue lines representing strike orientations of fractures were derived by visual interpretation. 21
- Figure 4.2** Rose diagram showing fracture orientation and frequency in western area of Thep sathit district derived by visual interpretation. Showing three main fracture orientations: NW-SE, NE-SW and N-S trend. 22
- Figure 4.3** Rose diagram showing fracture orientation and frequency in western area of Thep Sathit district derived by Mesh selection analysis. Showing three main fracture orientations: NW-SE, NE-SW and N-S trend. 22
- Figure 4.4** Digital outcrop model of Phasudpandin. Light blue, dark blue and orange lines representing N-S, NE-SW and WNW-ESE strike orientations of fracture respectively, are derived by visual interpretation. 23
- Figure 4.5** Rose diagram showing fracture orientation and frequency in western area of Thep sathit district derived by visual interpretation. Showing three main fracture orientations: NW-SE, NE-SW and N-S trend. 24
- Figure 4.6** Rose diagram showing fracture strike orientation and frequency of Phasudpandin derived by Mesh selection Analysis. Showing three main fracture orientations: NNW-SSE, NE-SW and NNE-SSW. 24

Figure 4.7	Digital outcrop model of Pahinngam national park. Light blue, dark blue and orange lines representing N-S, NE-SW and NNW-SSE strike orientations of fracture respectively, are derived by visual interpretation.	25
Figure 4.8	Rose diagram showing fracture strike orientation and frequency of Pahinngam national park derived by visual interpretation. Showing two main fracture orientations: NE-SW and N-S.	26
Figure 4.9.	Rose diagram showing fracture strike orientation and frequency of Thep Phana waterfall in Thep sathit district. Showing three main fracture orientations: WNW-ESE, ENE-WSW and N-S	26
Figure 4.10	Rose diagram showing fracture strike orientation and frequency of Thep Prathan waterfall in Thep sathit district. Showing three main fracture orientations: WNW-ESE, ENE-WSW and N-S.	27
Figure 4.11	Three directions of fracture in Thep Phana waterfall	28
Figure 4.12	WNW-ESE trending dextral strike-slip fracture in Thep Phana waterfall showing slickensides along fracture plane.	28
Figure 4.13	WNW-ESE trending dextral strike-slip fracture in Thap Prathan waterfall showing slickensides along fracture plane.	29
Figure 4.14	WNW-ESE trending dextral strike-slip fracture in Wat Nam Tok Charoen Tham showing slickensides along fracture plane.	29
Figure 4.15	ENE-WSW trending sinistral strike-slip fracture in Thep Phana waterfall showing slickensides along fracture plane.	30
Figure 4.16	ENE-WSW trending sinistral strike-slip fracture in Phasudpandin showing slickensides along fracture plane.	30
Figure 4.17	ENE-WSW trending sinistral strike-slip fracture in Wat Nam Tok Charoen Tham showing slickensides along fracture plane.	31

Figure 4.18	ENE-WSW trending sinistral strike-slip fracture in Thep Phana waterfall showing slickensides along fracture plane.	31
Figure 4.19	ENE-WSW trending sinistral strike-slip fracture in Thep Prathan waterfall showing slickensides along fracture plane.	32
Figure 4.20	N-S trending open fracture in Thep Phana waterfall showing no evidence for movement along fracture plane.	32
Figure 4.21	N-S trending open fracture in Phasudpandin showing no evidence for movement along fracture plane.	33
Figure 4.22	N-S trending open fracture in Wat Nam Tok Charoen Tham showing no evidence for movement along fracture plane.	33
Figure 4.23	2D stress ellipse showing types and trends of fracture, the dihedral angle and range of σ_1 direction.	34
Figure 5.1	Digital elevation model of Thep Sathit showing wester area has high elevation than eastern area.	37
Figure 5.2	Snistral strike-slip fault along western margin of Khorat plateau and reverse fault in western area of district are resulted from N-S compression.	38
Figure 5.3	Conceptual model for fracture development showing fracture, high elevation area in western part of Thep Sathit district and sinistral strike-slip fault are resulted from N-S compression in Paleogene.	39

Chapter 1

Introduction

1.1 Introduction

Fracture which is one of the type of deformation formed when stress applied on the rock is more than the rock strength. Fracture orientation and type of fracture depend on the stress state. Therefore, fracture analysis can describe state of stress at the moment of fracturing.

Phasudpandin is tourist attraction in Thep Sathit District, Chaiyaphum Province. There are two remarkable features. One is clear exposure of cliff and the other is there is systemic fractures scattered throughout the cliff. Geological event, that is cause of cliff lifting, is described on a board in Phasudpandin. Unfortunately, the content on the board is wrong and there is no explanation about the systematic fracture. In large scale, digital elevation model (DEM) shows there are many fractures or lineaments along western part of Thep Sathit that seem to be related with systematic in Phasudpandin. This area is on a Phra Wihan formation that deposited in Early Crataceous. Fracture analysis will point out which stress applied on the study area after Early Cretaceous period is responsible for these fractures.

The main objectives of this study are to create fracture map and to propose a conceptual model for fracture development in Khorat Group, Thepsatit District, Chaiyaphum Province by using field observation, digital outcrop model (DEM) and digital outcrop model (DOM).

1.2 Study area

Study area is Thep Sathit district, Chaiyaphum province that located on western margin of Khorat plateau (Fig 1.1). The total area is approximately 875.6 square kilometers. Due to fractures are particularly distributed on western part of Thep Sathit, all field study is on along western part of Thep Sathit district, Chaiyaphum province. Field study investigated in cliff top land or Phasudpandin, Pahinngam national park, Thep Phana waterfall, Thep Pratan waterfall and Wat Nam Tok Charoen Tham.

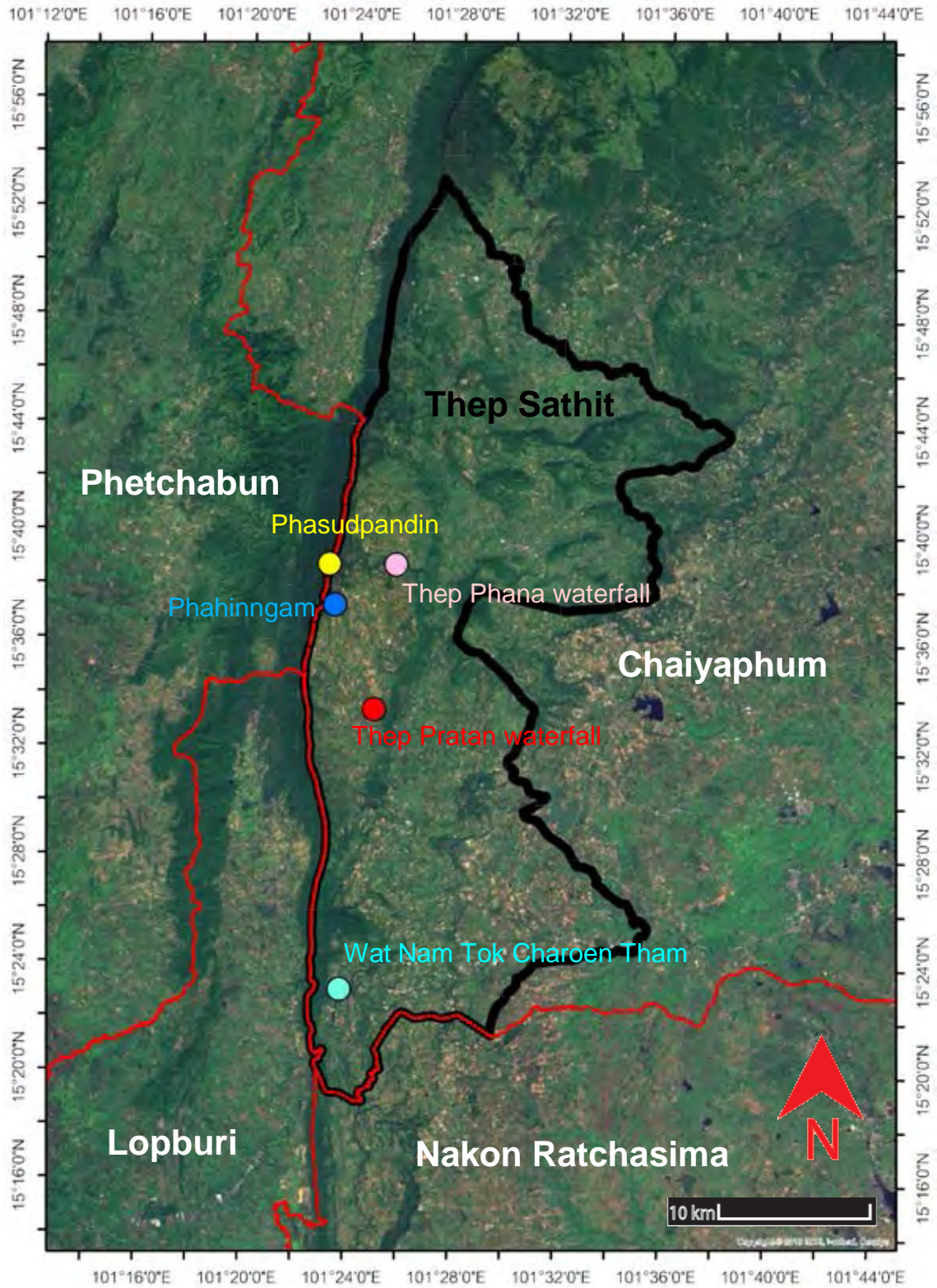


Figure 1.1 Satellite image showing boundary of Thep sathit district, and location of field observation.

Chapter 2

Geological Background

2.1 Stratigraphy

Thep Sathit district concludes 4 formations of Khorat Group: Phra Wihan formation, Sao Khua formation, Phu Phan formation and Krok Kruat formation, respectively from old to young (Fig 2.1, 2.2).

Phra Wihan formation is widely distributed around western margin of Khorat plateau. This formation mainly comprises of fine to coarse grained quartzitic sandstones and rarer mudstones and siltstones with occasional conglomerates (A.Meesook, 2011). The Phra Wihan formation is of Berriasian-Barremian age (Early Cretaceous) that suggested by and Racey & Goodall (2009).

Sao Khua formation comprises of reddish-brown conglomeratic sandstone, siltstone and mudstone. At the base, rock comprise of reddish-brown silty claystones, siltstones and fine to medium-grained sandstones with thin calcrete horizons and some silcrete layers (A.Meesook, 2011). The Sao Khua formation is of Berriasian-Barremian age (Early Cretaceous) that suggested by Racey & Goodall (2009).

Phu Phan formation comprises of greyish-white medium to coarse grained cross-bedded sandstones and thin lenses of grey siltstone and mudstone with subordinate conglomerate (A.Meesook, 2011). The Phu Phan formation is of Berriasian to Aptian age (Early Cretaceous) that suggested by Racey & Goodall (2009).

Krok kruat formation comprises of reddish-brown fine to medium grained sandstone, siltstone and mudstone with some conglomerate beds (A.Meesook, 2011). The Krok kruat formation is of Aptian age (Early Cretaceous) that suggested by Racey & Goodall (2009).

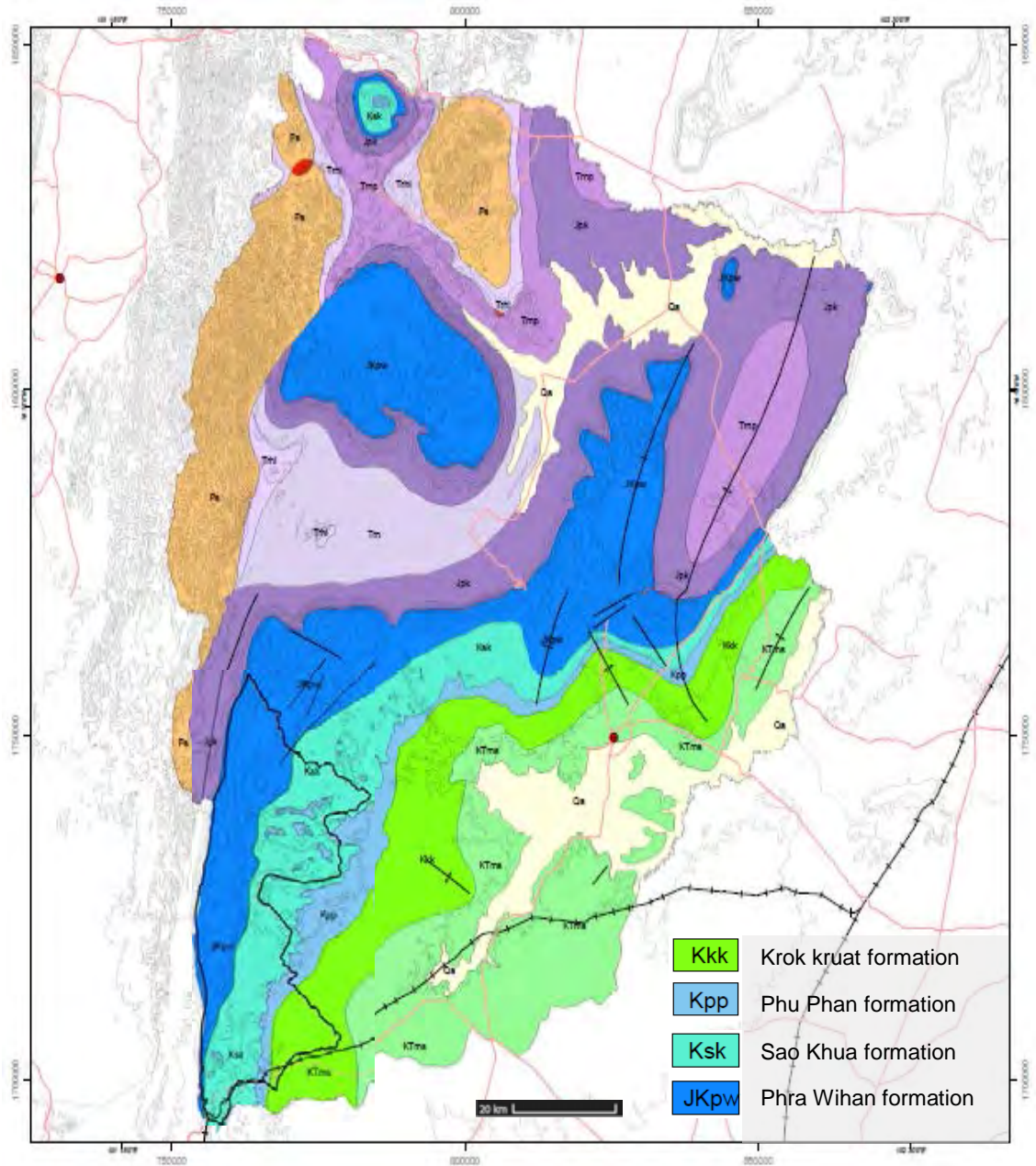


Figure 2.1 Geological map of Chaiyaphum province, black line represent Thep sathit boundary (modified after DMR, 2007)

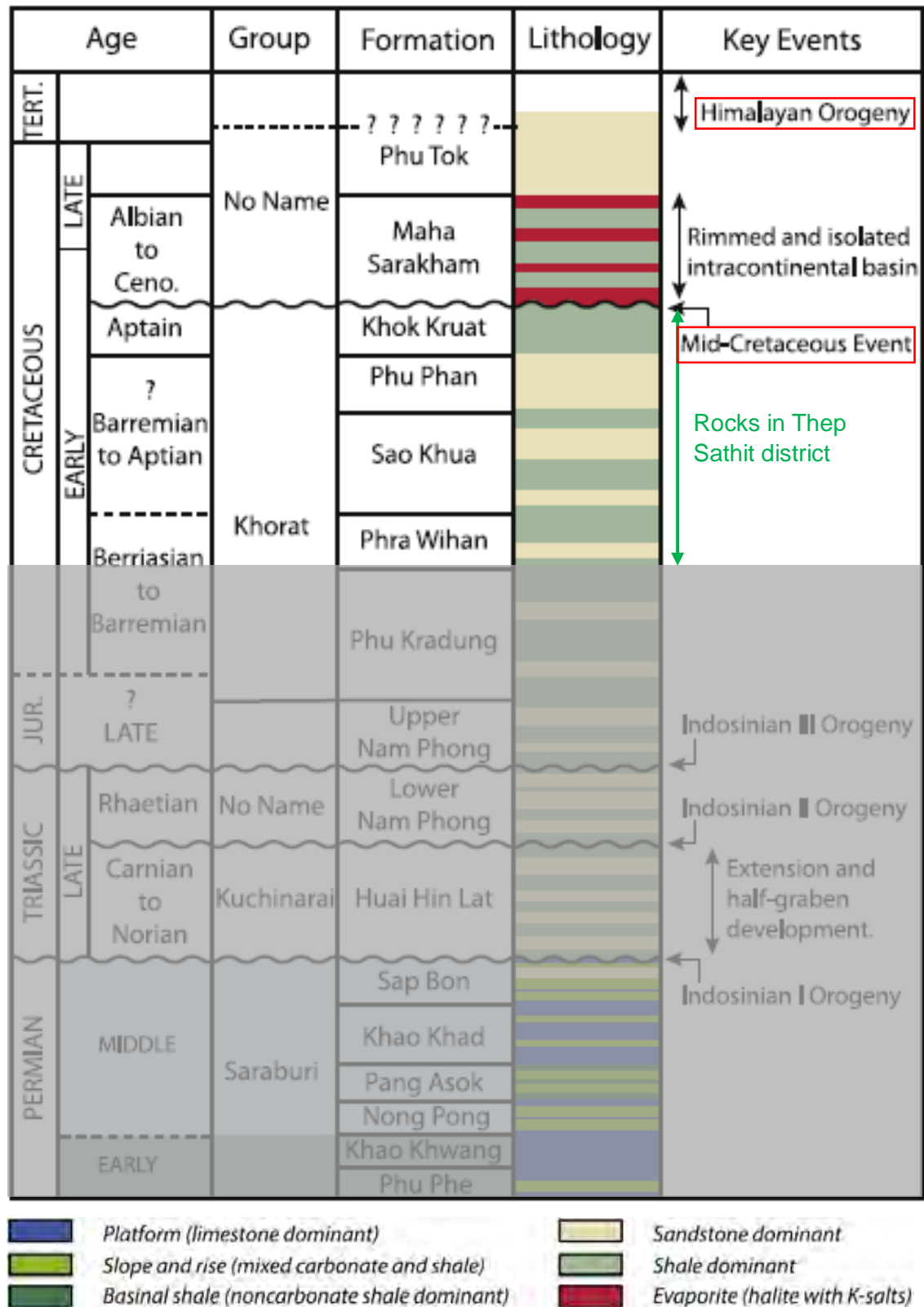


Figure 2.2 Regional stratigraphy shows Lithology, sequence of rocks, age of rock and key events during Permian to Tertiary. Rocks in study area is in Cretaceous age. The red rectangular frame emphasize two tectonic events after deposition of rock in study area (modified after Warren et al., 2014).

2.2 Geological setting

Khorat Group was deposited during Late Jurassic and Early Tertiary. There are two interpretations for deposition of Khorat Group. One is the model most frequently applied to the area is that of Cooper et al. (1989), who interpreted that the Khorat Group was deposited in a thermal sag basin following Late Triassic extension related to Indosinian Orogeny. The other is more recently is that of Lovatt-Smith et al. (1996), who suggested that Khorat Basin was a foreland basin at the front of a Jurassic Orogenic belt created by the Song Ma and Song Da sutures which parallel the axis of Khorat Basin and is a suture between the South China Block and Indochina. The top of the Khorat Group is marked by an unconformity that separated the Aptian Khok Kruat Formation from the Albian–Cenomanian continental evaporitic Maha Sarakham Formation.

The top of the Khorat Group is marked by an unconformity between the Aptian Khok Kruat Formation and the Albian–Cenomanian continental evaporitic Maha Sarakham Formation. This unconformity represents a mid-Cretaceous inversion. P.F. LOVATT SMITH et al. (1996) suggested that Mid-Cretaceous inversion is caused by continental collision to the west, such as collision of West Burma with Sibumasu which is stated by Metcalf (1996) and N.J. Gardiner et al. (2016). This inversion resulted in development of Phu Phan uplift (Racey, 2009), uplift in western area of Khorat plateau (Booth, 1998) and folded area in Khorat plateau (Booth and Sattayarak, 2011). Moreover, it led to development of rimmed intracratonic basin into that Maha Sarakham Formation was deposited. Himalayan Orogeny is caused by India plate colliding with Eurasia plate in Middle Eocene age (Morley, 2012) (Fig 2.3d). In Middle Eocene, it occurs transpression, folding, thrusting and erosion of Khorat Group (Searle & Morley, 2011).

2.3 Fracture type

Fractures can be separated into opening or extension fracture (joint, vein and fissure) and shear fractures. Additionally, closing or contraction fractures can be determined (stylolite). Shear fracture has sense of displacement parallel to the fracture plane. Opening or extension fracture has sense of displacement perpendicular to fracture plane. Joint has no or little displacement across the fracture plane. The term Vein is used for mineral-filled extension fracture. Air or fluid-filled extension fracture is called fissure (Fig 2.4). In this study, fractures are separated into 3 types: shear fracture, extension fracture and contraction fracture.

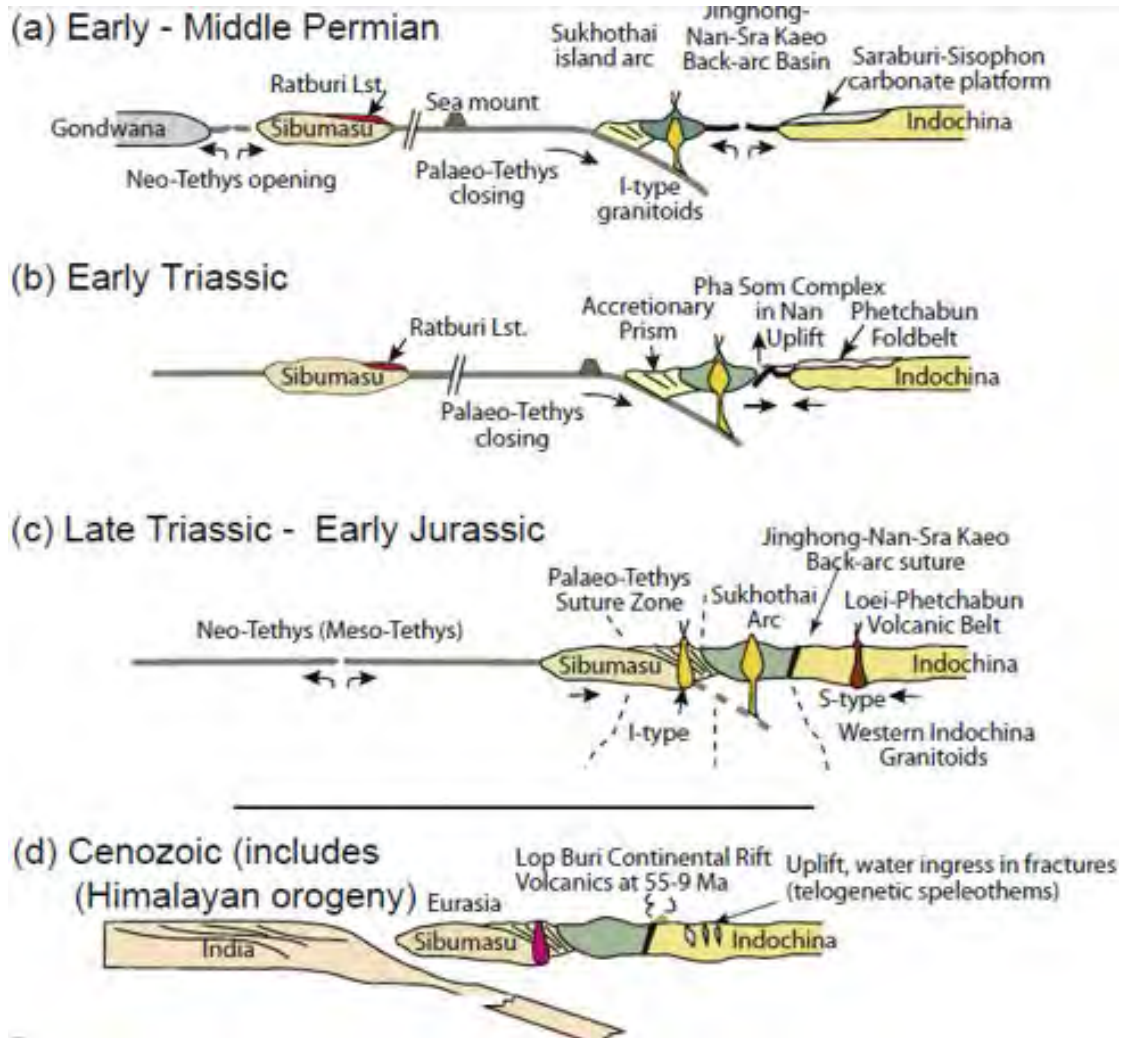
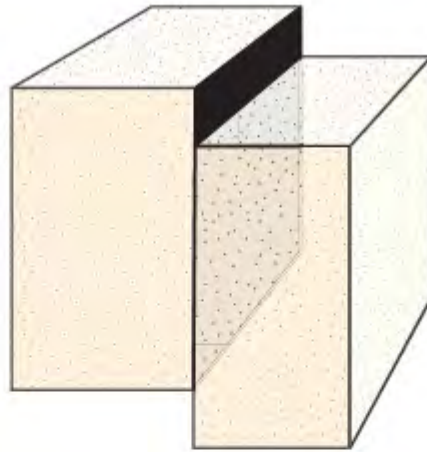


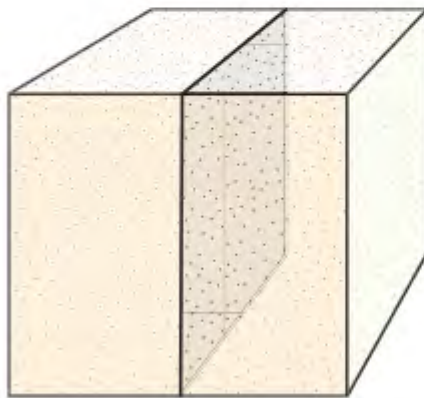
Figure 2.3 Tectonic evolution of Thailand from Late Palaeozoic to Cainozoic (Warren et al., 2014).

2.4 Dihedral angle

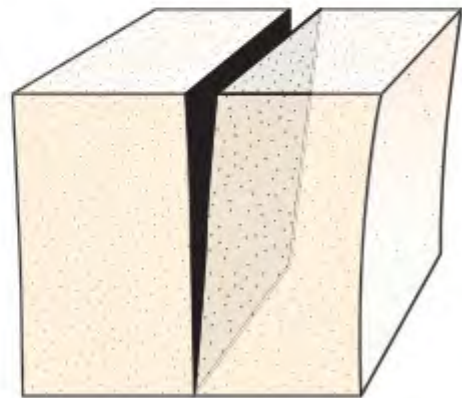
A dihedral angle is angles between dihedral shear fracture. According to Mohr-Coulomb theory, the dihedral angle is normally about 60° or acute angles. But according to Paacock & Sanderson (1995) and Ismat (2015), the dihedral angle can be unusually large. Paacock & Sanderson (1995) stated that high dihedral angle (often $>90^\circ$) is the evidence of pressure solution in rock. Ismat (2015) showed the dihedral angle increases with increasing confining pressure which will be increased when the rock is in deep crust or close to the hinge regions of the folds. Moreover, Ismat stated that the maximum principle stress directions based on the acute bisectors of conjugate-fractures may not be accurately determined if the dihedral angle is unusually large or small, leading to incorrect kinematic analyses.



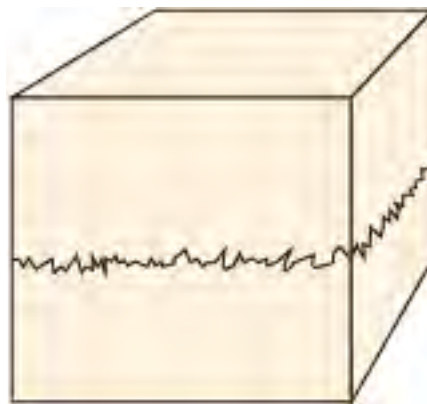
Shear fracture



Extension fracture:
Joint



Extension fracture:
Fissure



Contraction fracture

Figure 2.4 The types of fracture.

Chapter 3

Methodology

This chapter consists of four parts. The first part is data collection. The second part shows a methodology for making digital outcrop models. The third part presents the fracture analysis for determining stress state. The last part is the stress analysis. The work flow is shown in Figure 3.1.

3.1 Data collection

Digital elevation model (DEM), digital outcrop model (DOM) and field data are used to analyze fracture orientations and stress state in this study. Fracture strikes are obtained from DEM, DOM and field data while dips and types of fracture are obtained only from field data.

DEM is 12.5 meter resolution from Alaska Satellite Facility. Dataset's name is ALOS PALSAR. The Pashit district is combined with 4 pairs of path and frame: path:484 frame:300, path:484 frame:290, path:485 frame:300 and path:485 frame:290.

In Pashupandin and Pashingam national park, DOM must be used to study fractures because these outcrops are large and difficult to access. DOM is constructed from outcrop photos, so outcrop photos are one of the data that needs to be collected. Outcrop photos are collected by capturing photos and recording some geological references.

The significant field data are fracture strike, fracture dip, fracture type, slickenlines trend and slickenlines plunge. A type of fracture is important for stress analysis.

3.2 Digital outcrop model construction

DOM is a digital 3D outcrop used for analysis and measurement of some geological features e.g. orientation of geological surface or structure, width and thickness of layers. The amount of identifiable and measurable geological features highly depend on the resolution and accuracy of DOM. In this study, DOM is created by Agisoft Photoscan software. Input data for creating DOM is outcrop photos with geological reference coordinates. There are 4 procedures for creating DOM. The first procedure is camera alignment of series of overlapping outcrop images (Fig 3.2a). Then, software will generate a point cloud model (Fig 3.2b). After that, Triangles mesh will be created from the point cloud model (Fig 3.2c). The last procedure before exporting model is textured model building (Fig 3.2d).

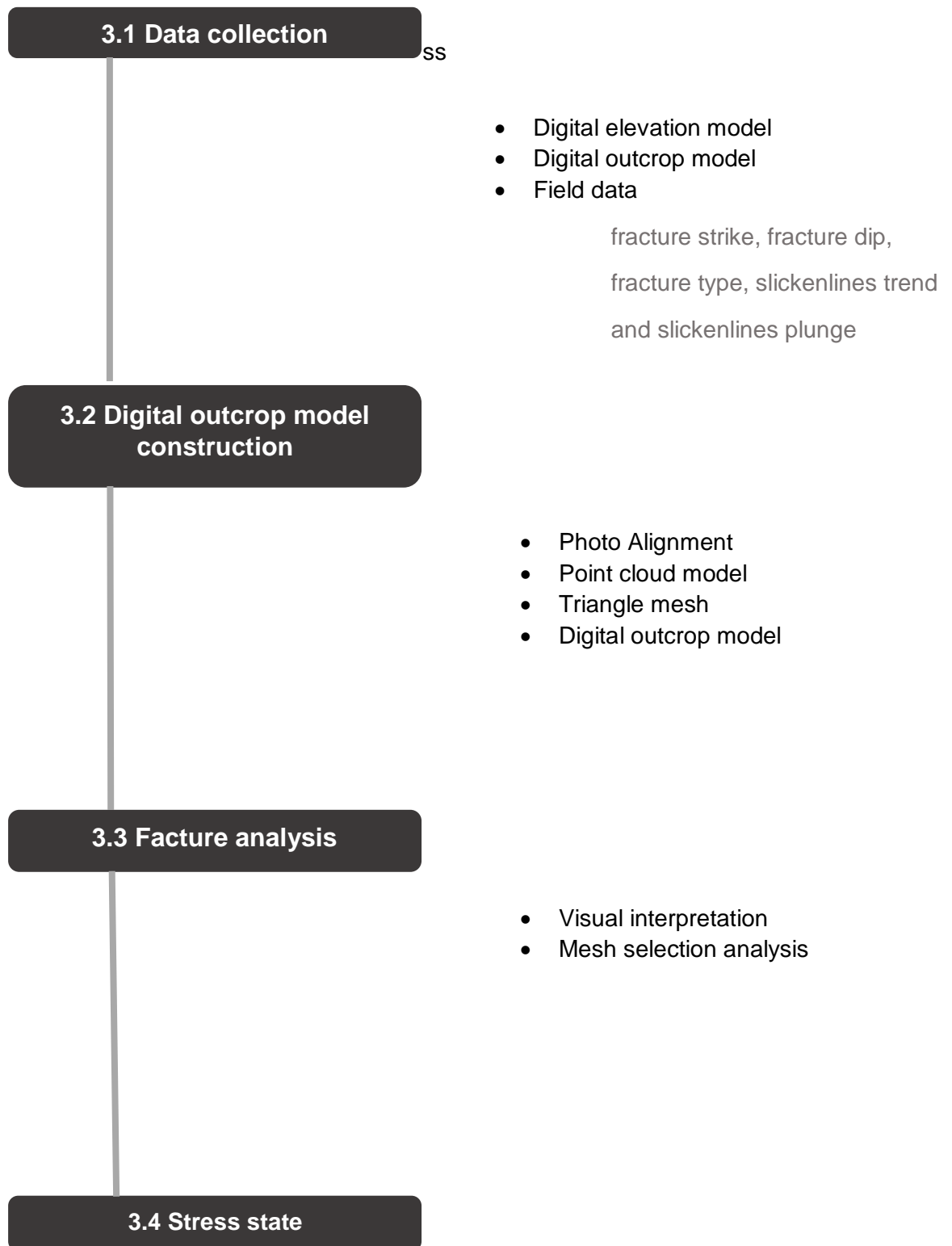
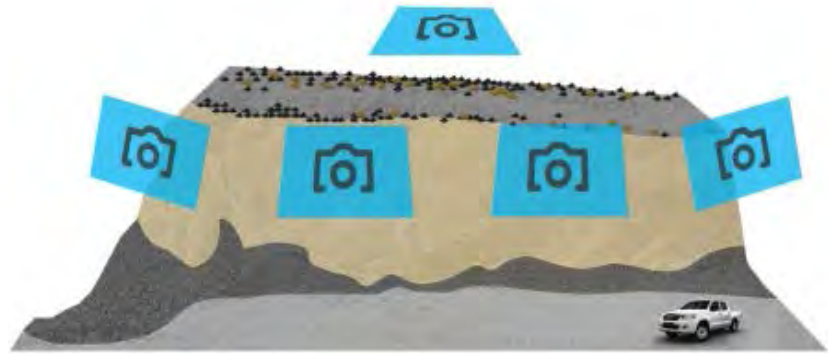


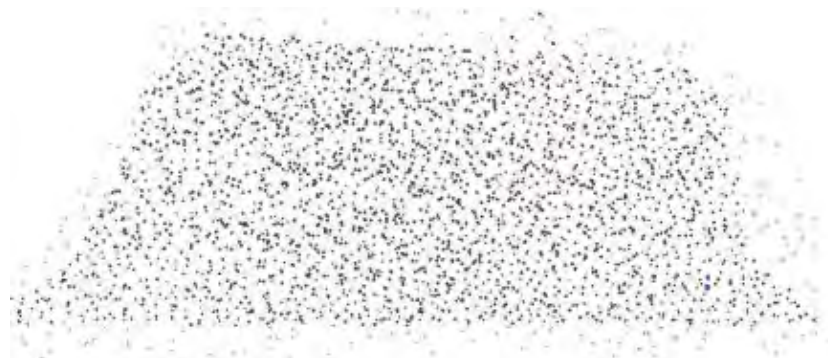
Figure 3.1 Methodology showing the four main stages of this study.

a) Align photos

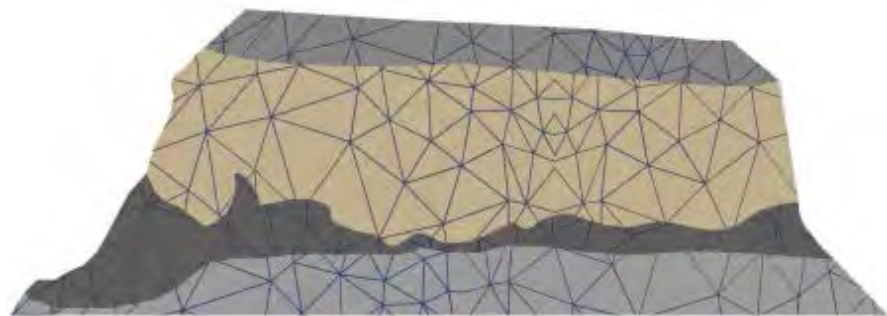
๙



b) Generate point cloud



c) Create Triangles mesh



d) Export Digital Outcrop Model



Figure 3.2 Four main procedures of Digital Outcrop Model construction by using Photoscan software (Jirapat, 2016).

3.3 Fracture analysis

There are two methods for fracture analysis: visual interpretation and mesh selection analysis.

3.3.1 Various directional sun azimuth in DEM

Difference of sun azimuth for visual interpretation in DEM affects the frequency of each fracture trend. Generally, frequency of fracture trend, perpendicular to the sun azimuth, is dominant. So, using one directional sun azimuth to analyze fracture orientation may cause misunderstanding about frequency of fracture (Masoud & Koike, 2017). This study uses various directional sun azimuth to avoid this problem (Fig 3.3). Then, fractures from each sun azimuth, are gathered in one picture shown in figure 4.1

3.3.2 Mesh selection analysis

This study uses the triangles mesh to analyze fracture orientations. The triangles mesh was created from linking three points in the photo. Each point has geological reference coordinates, which results in three dimensional orientation of each triangles mesh. Therefore, we use triangles meshes to represent the fracture orientation. In this study, input data for mesh selection means are DOM and DEM. DOM is already mesh but DEM isn't. So, before being processed, DEM must be converted from grid to mesh. There are two processes for Mesh selection means. The processes begin with creation of dip attribute (Fig 3.4). Mesh occurring around fractures plane usually has steeper dip angle than meshes in nearby area (Fig 3.5). Hence, to analyze fracture trend, meshes which are not representative of fractures have to be exterminated by determining unwanted dip angles. Then, unwanted dip angles will be selected and deleted (Fig 3.6). The last step is the creation of azimuth attribute of the rest meshes to show direction of them (Fig 3.7).

3.4 Stress Analysis

Fractures in rock are caused by stress. Types and orientations of fracture depend on direction of principal stress. Therefore, fracture analysis can describe state of stress at the moment of fracturing. Generally, fractures are classified into 3 types: shear fracture, extension fractures and contraction fracture. The shear fractures form some acute angle to the maximum compressive principle stress direction (σ_1). An angle between conjugate shear fractures is called dihedral angle. The extension fractures form perpendicular to minimum compressive principle stress direction (σ_3). The contraction fracture form perpendicular to σ_1 and parallel to σ_3 . σ_1 direction can be generally identified by two means. First, maximum compressive principle stress direction is parallel to extensional fracture plane. Second, maximum compressive principle stress direction is parallel to bisector of conjugate angle. (Fig 3.8)

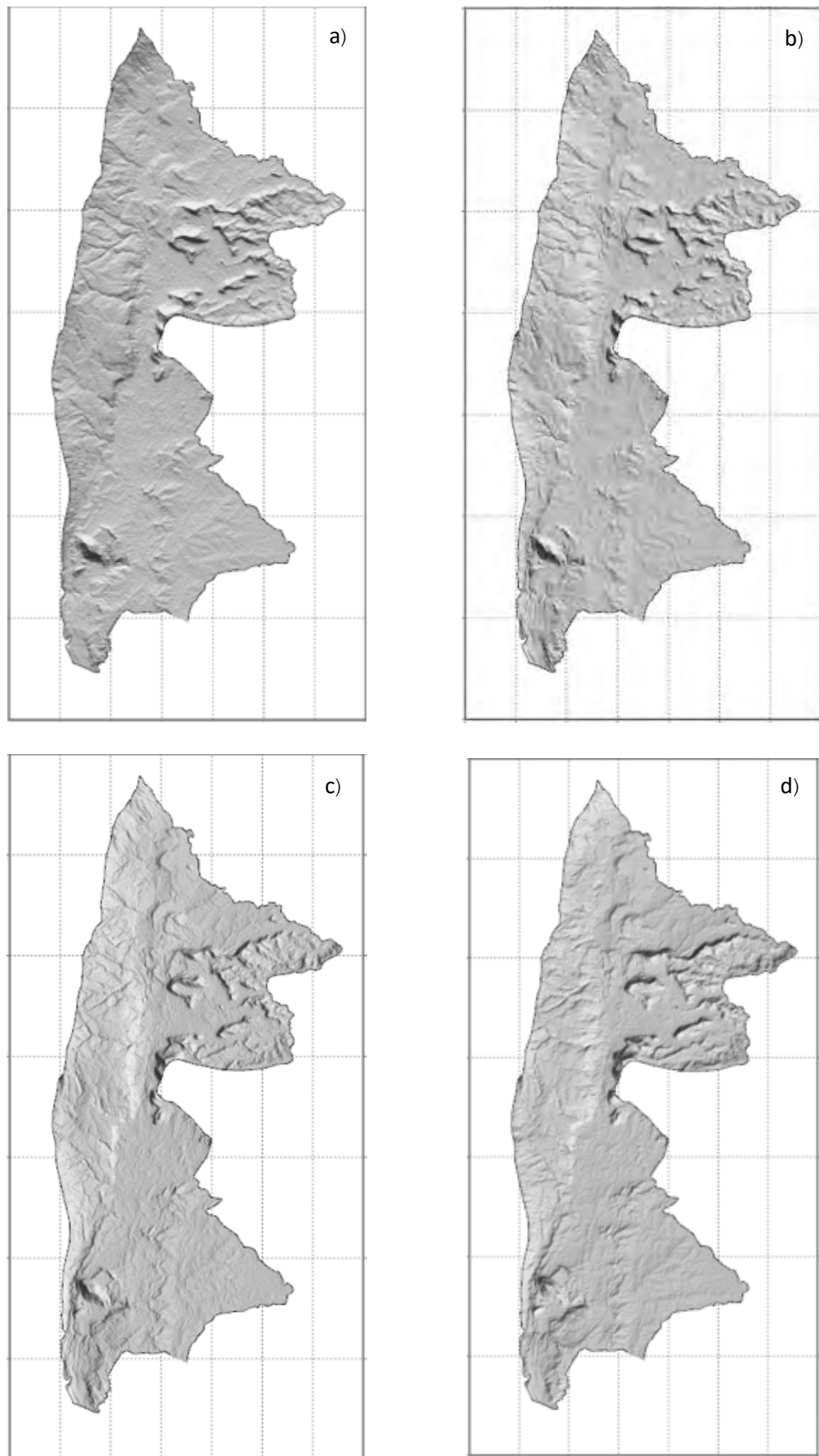


Figure 3.3 Variation of sun azimuth, a) N-S direction, b) NE-SW direction, c) E-S direction and d) SE-NW direction, showing different in fracture intensity.

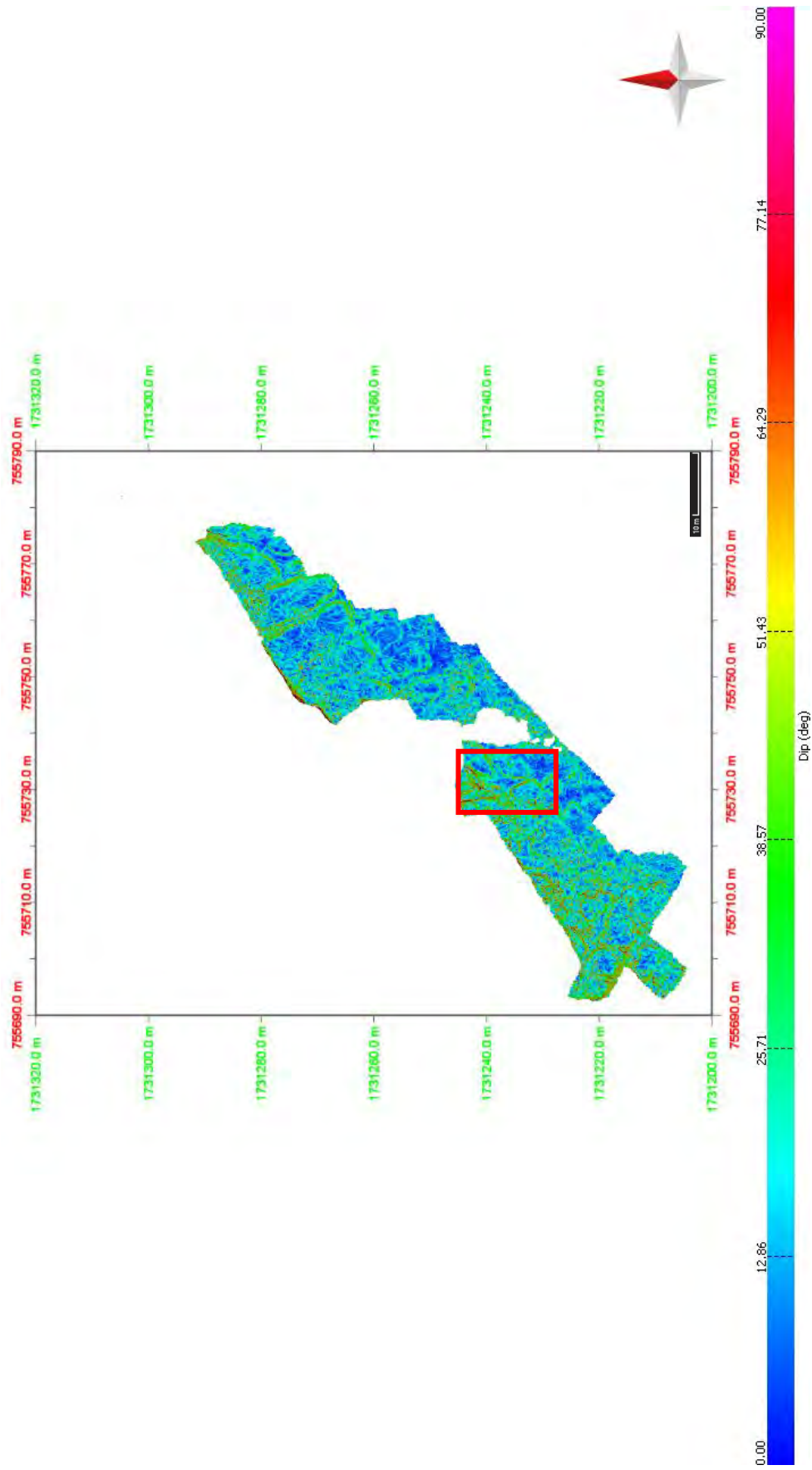


Figure 3.4 Dip attribute showing all various dip angles of mesh in Phasudpandin. The red rectangular frame showing location of figure 3.5.

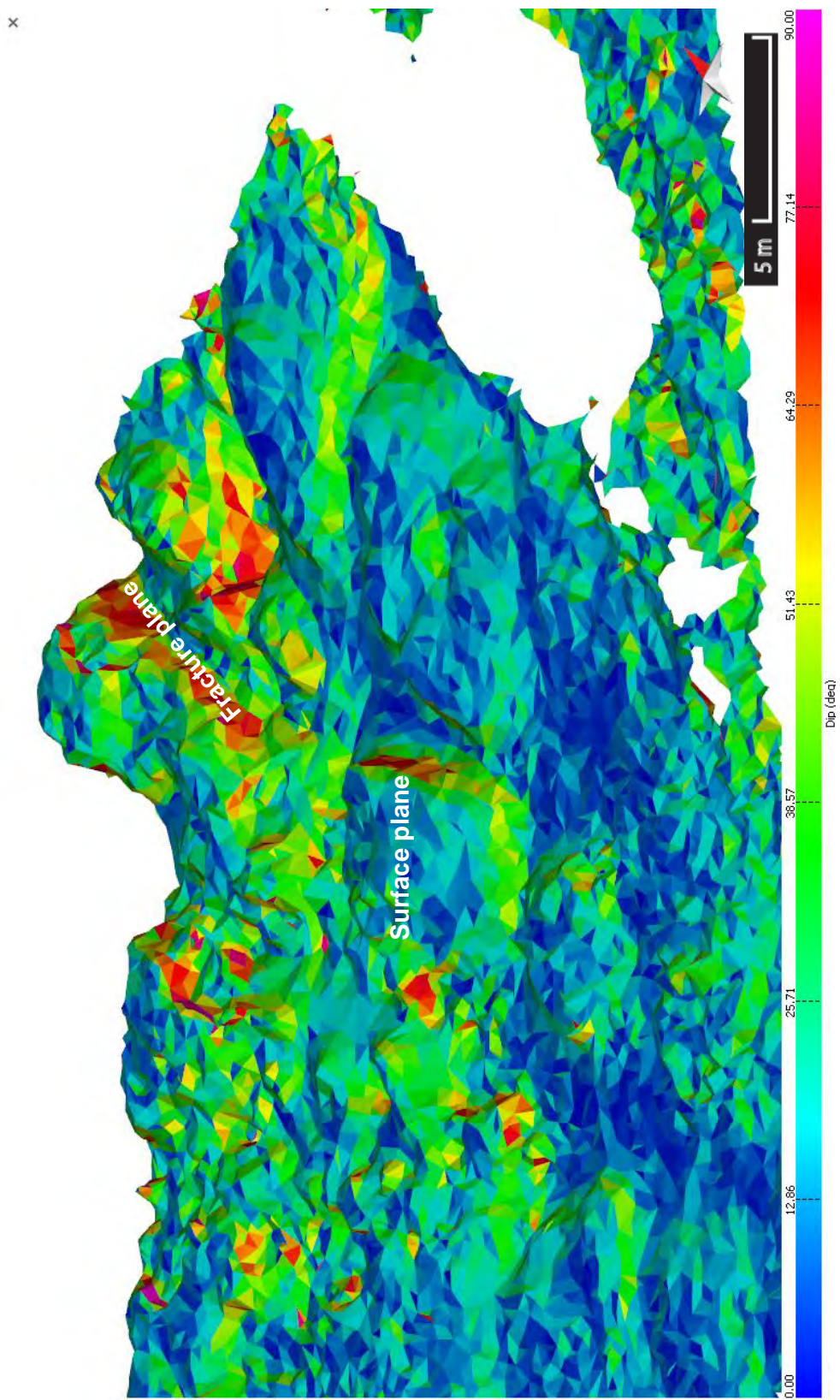


Figure 3.5 Showing dip angle on fracture plane (red area) higher than surface plane.(blue area).

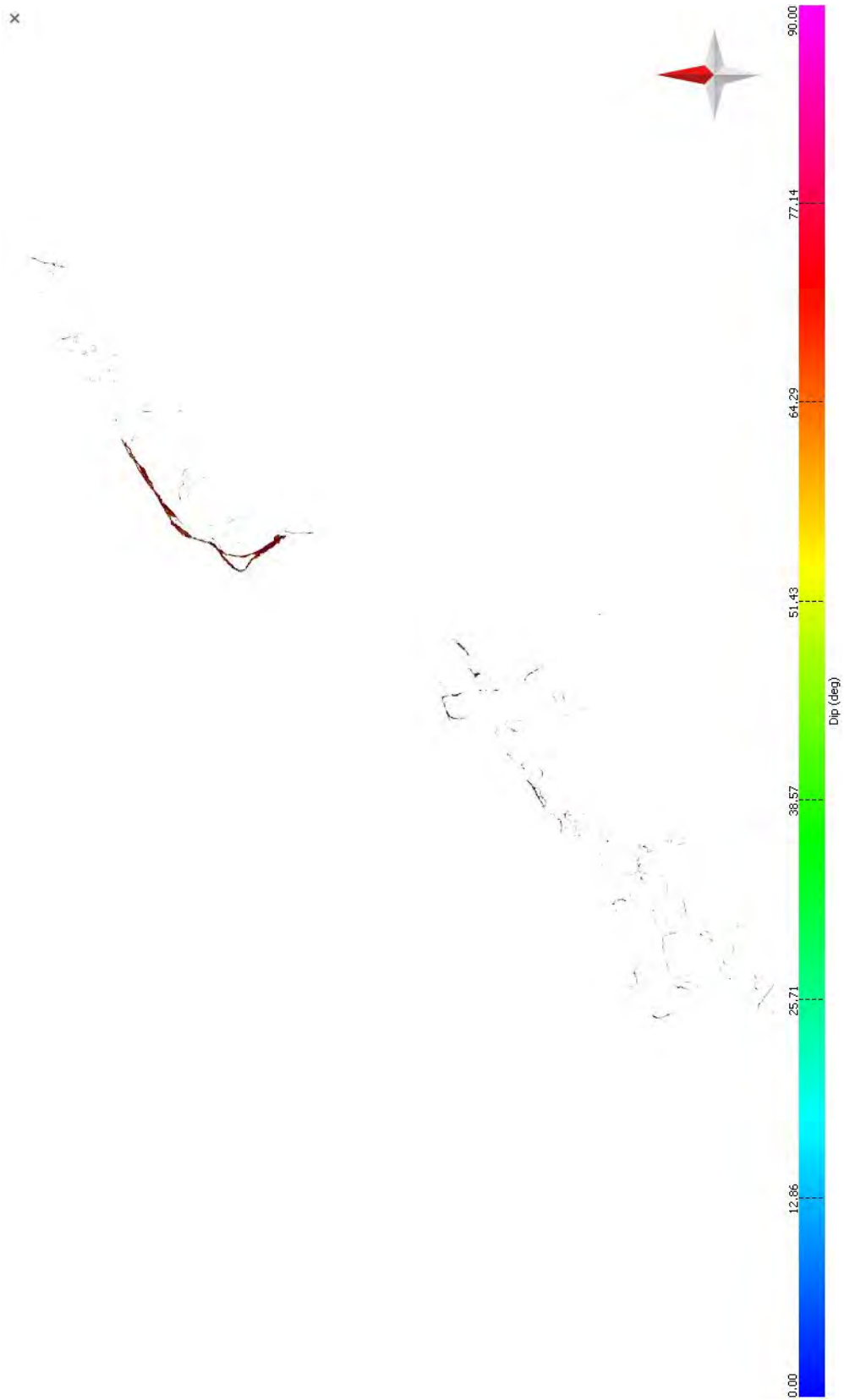


Figure 3.6 The rest meshes (dip>60°) representing fracture orientation in Phasudpandin.

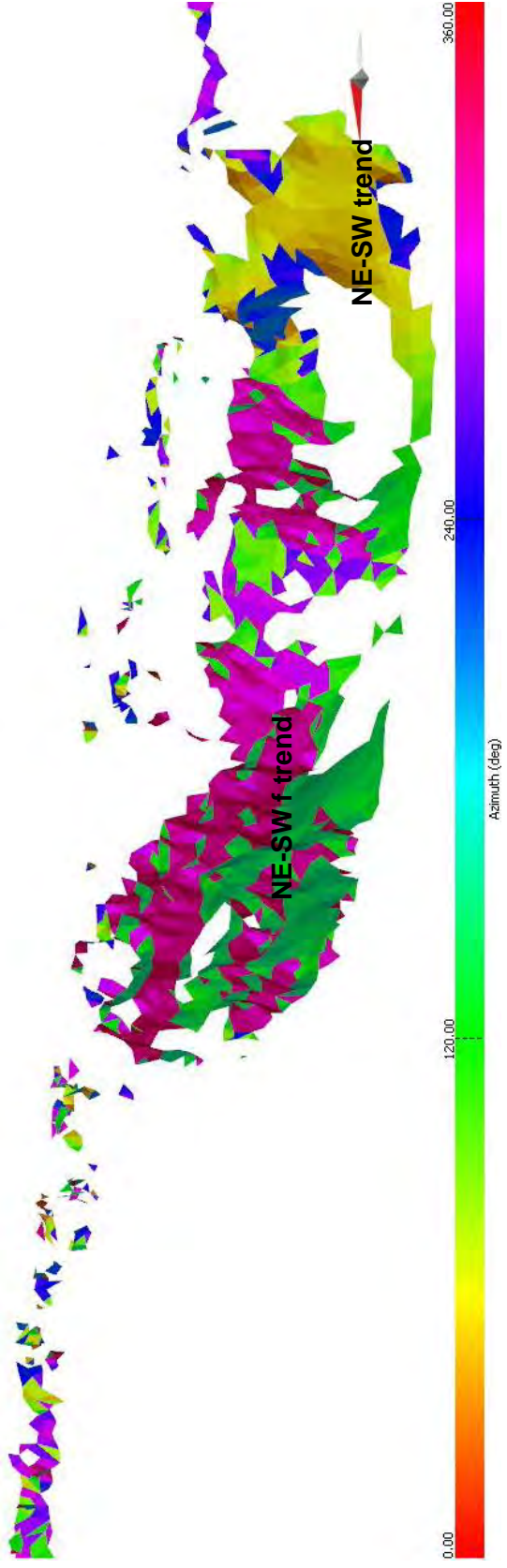


Figure 3.7 Azimuth of rest mesh showing the different mesh colour in each fracture trend. Purple meshes representing NE-SW fracture trend. Yellow meshes representing NW-SE fracture trend. Showing variation of colour or mesh orientation in one fracture..trend. NE-SW has some green meshes and NW-SE has some blue meshes.

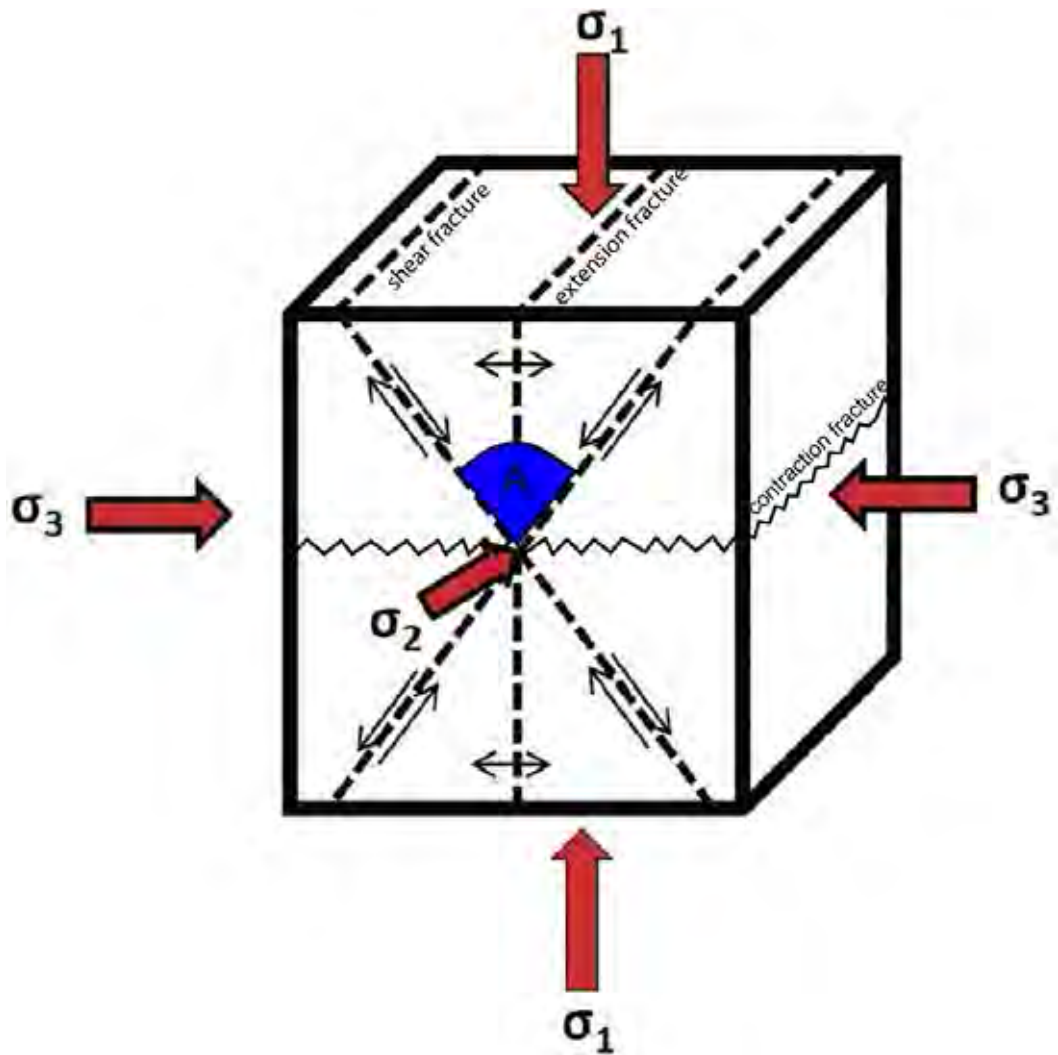


Figure 3.8 Relationship of principle stresses, Extension fracture , Shear fracture, maximum principle stress (σ_1), intermediate principle stress (σ_2), minimum principle stress (σ_3) and A: Dihedral angle.

Chapter4

Result

4.1 Fracture orientation

Fracture orientations in this study are derived from Digital elevation model, Digital outcrop model and Field observation.

4.1.1 Digital elevation model

- Visual Interpretation

Fracture locations in western area of Thep sathit district, that derived from visual interpretation, are showed in Figure 4.1. The strike orientations of fractures lie in NW-SE direction and range from 300 to 310 degrees, NE-SW direction range from 50 to 60 degrees, N-S direction range from 340 to 10 degrees and E-W direction range from 270 to 280 (showed in rose diagram of Fig 4.2)

- Mesh Selection Analysis

There are 4 main strike orientations of mesh: NW-SE direction ranging from 310 to 320 degrees, NE-SW direction ranging from 40 to 60 degrees, N-S direction range from 340 to 10 degrees and E-W direction range from 260 to 290 (showed in rose diagram of Fig 4.3).

4.1.2 Digital Outcrop Model

Digital Outcrop Model of Phasudpandin (UTM: 755753.94, 1731303.96)

- Visual Interpretation

Visual interpretation DOM of Phasudpandin is showed in Figure 4.4. There are 3 main strike orientations of fractures: WNW-ESE direction ranging from 290 to 310 degrees, NE-SW direction ranging from 50 to 60 degrees and N-S direction ranging from 0 to 10 degrees (showed in rose diagram of Fig 4.5).

- Mesh Selection Analysis

Mesh selection analysis of Phasudpandin, shows 3 main strike orientations of meshes considering meshes that have dip higher than 75 degrees: NNW-SSE direction ranging from 320 to 340 degrees, NE-SW direction ranging from 40 to 60 degrees and NNE-SSW direction ranging from 10 to 20 degrees (showed in rose diagram of Fig 4.6).

Digital Outcrop Model of Pahinngam national park (UTM: 756194.48, 1728530.15)

- Visual Interpretation

There are 2 main strike orientations of fractures derived by visual interpretation DOM of Pahinngam national park (Fig 4.7). The strike orientations of fractures lie in NE-SW direction ranging from 50 to 60 degrees and N-S direction ranging from 0 to 10 degrees that are showed in rose diagram (Fig 4.8).

4.1.3 Field Observation

- Thep Phana waterfall (UTM: 759049.10, 1721489.93)

There are 3 main strike orientations of fractures from field observation in Thap Phana waterfall: WNW-ESE, ENE-WSW and N-S showed in rose diagram (Fig 4.9). WNW-ESE lie in the range of 290 to 300 degrees. ENE-WSW lie in the range of 60 to 70 degrees. N-S lie in the range of 0 to 10 degrees. Fractures in Thep Phana waterfall are subvertical(dip angle rage from 80 to 90 degrees (Fig 4.11)).

- Thep Prathan waterfall (UTM: 760299.72, 1731370.69)

There are 3 main strike orientations of fractures from field observation in Thap Phana waterfall: WNW-ESE, ENE-WSW and N-S showed in rose diagram (Fig 4.10). WNW-ESE lie in the range of 290 to 300. ENE-WSW lie in the range of 70 to 80 degrees. N-S lie in the range of 0 to 10 degrees. Fractures in Thep Prathan waterfall are subvertical (dip angle rage from 80 to 90 degrees (Fig 4.11)).

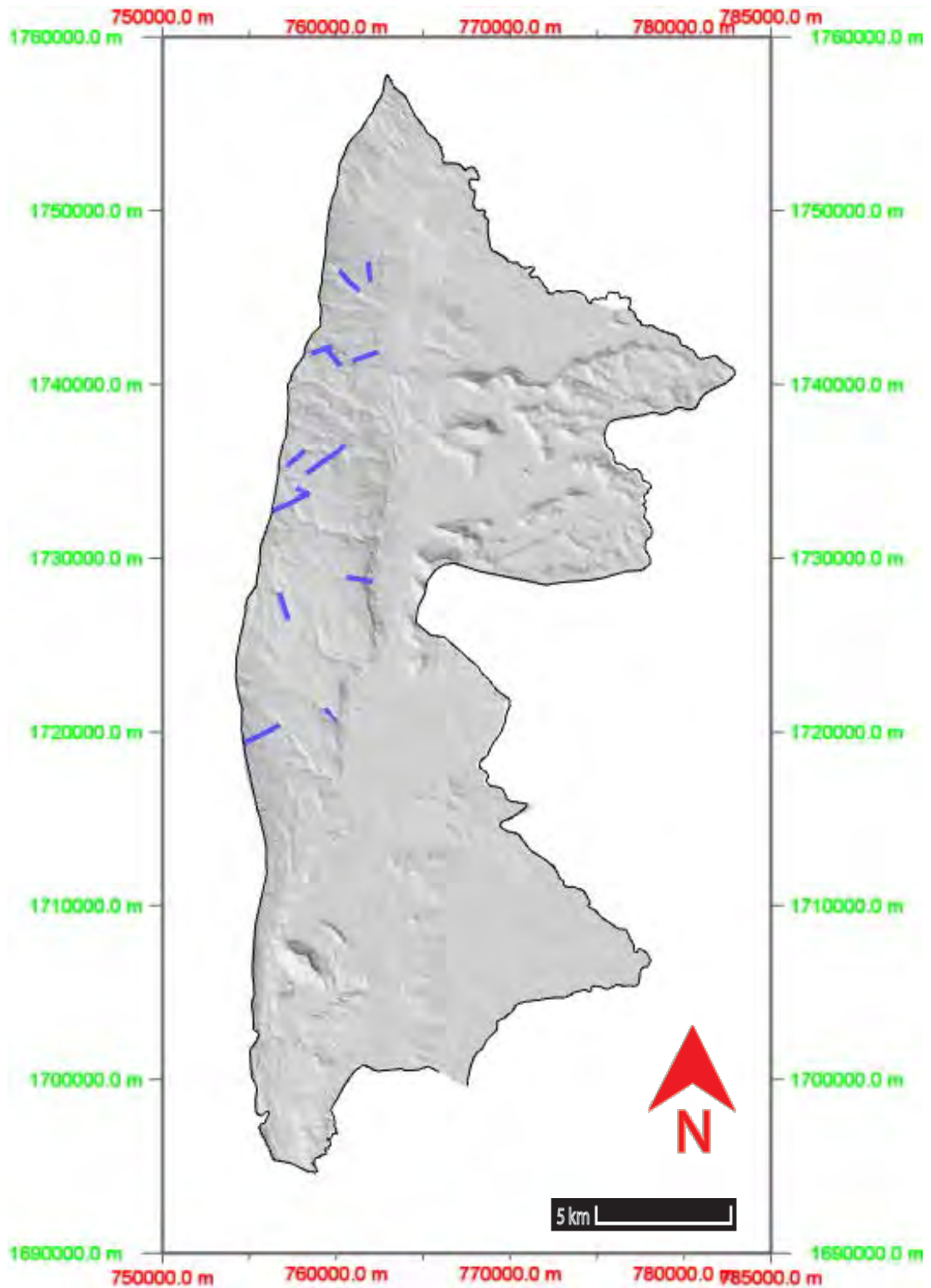


Figure 4.1 Digital elevation model of Thep sathit district. The blue lines representing strike orientations of fractures were derived by visual interpretation.

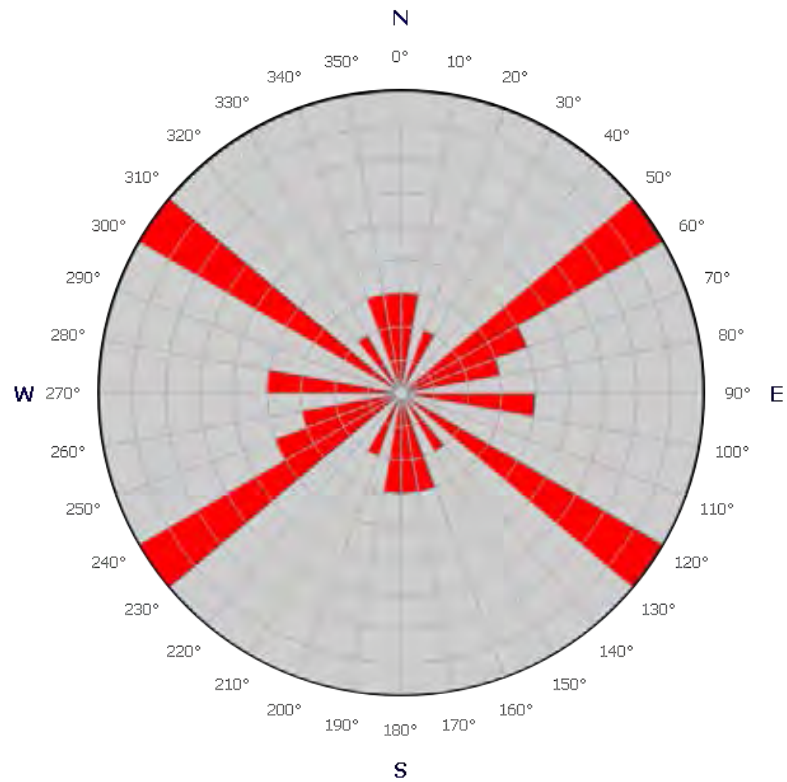


Figure 4.2 Rose diagram showing fracture orientation and frequency in western area of Thep Sathit district derived by visual interpretation. Showing three main fracture orientations: NW-SE, NE-SW and N-S trend.

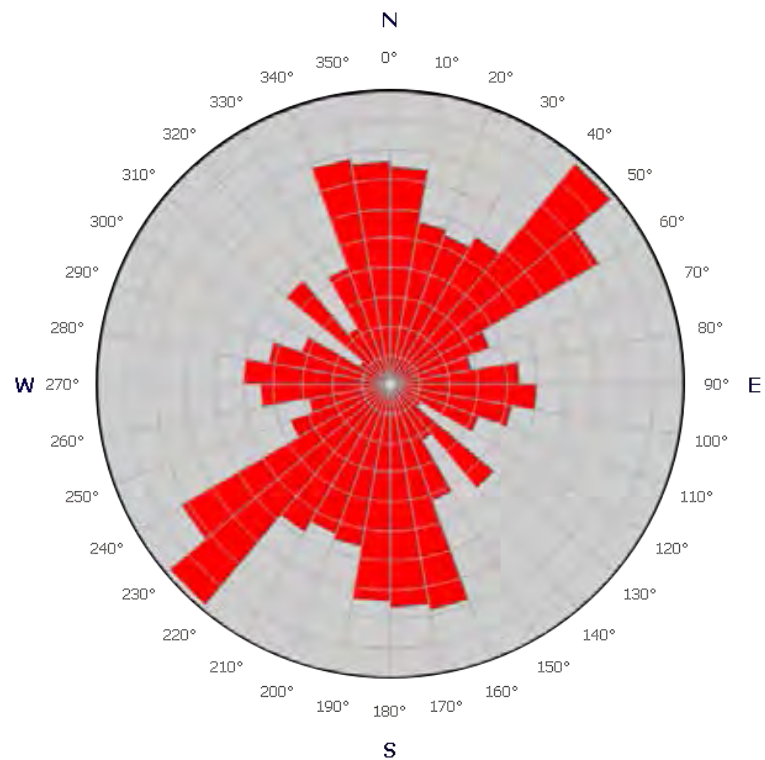


Figure 4.3 Rose diagram showing fracture orientation and frequency in western area of Thep Sathit district derived by Mesh selection analysis. Showing three main fracture orientations: NW-SE, NE-SW and N-S trend.

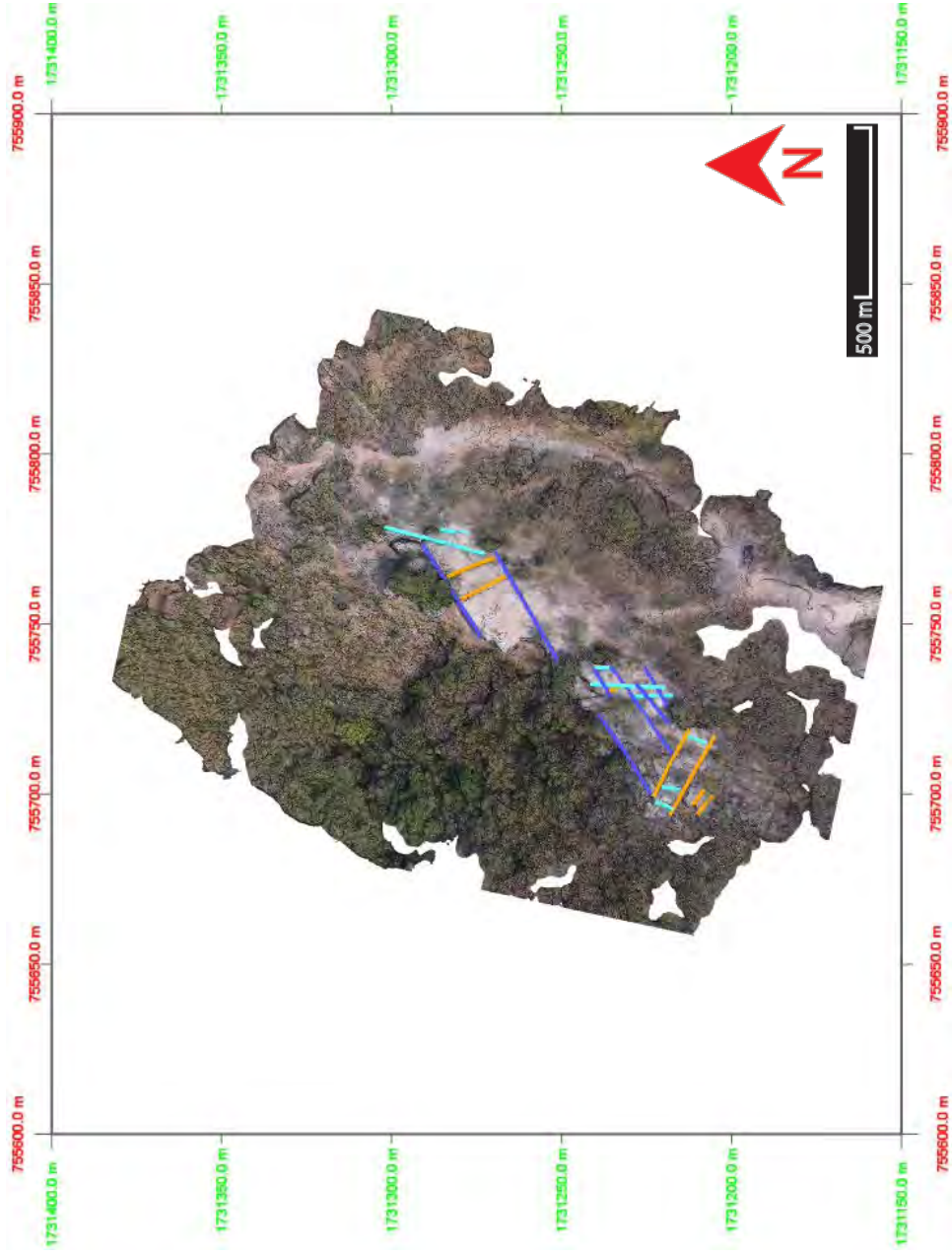


Figure 4.4 Digital outcrop model of Phasudpandin. Light blue, dark blue and orange lines representing N-S, NE-SW and WNW-ESE strike orientations of fracture respectively, are derived by visual interpretation.

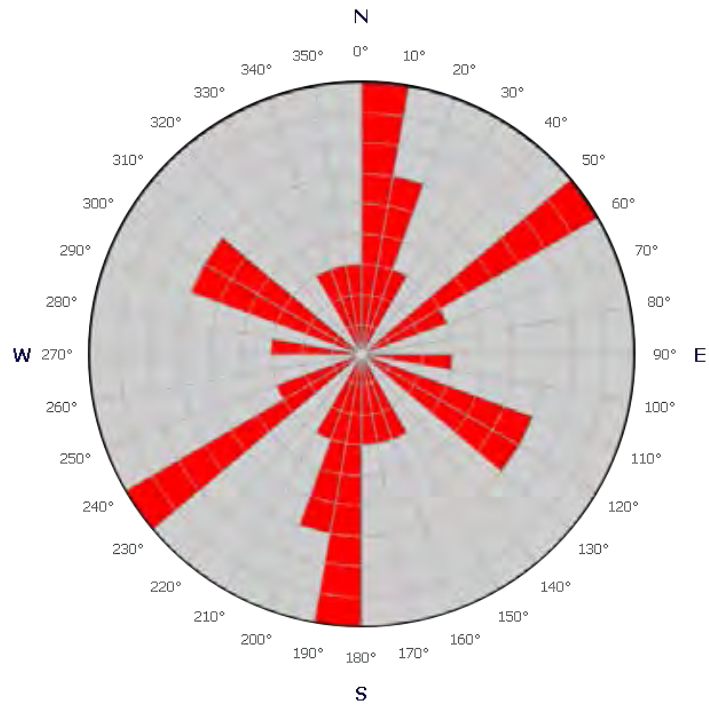


Figure 4.5 Rose diagram showing fracture strike orientation and frequency of Phasudpandin derived by visual interpretation. Showing three main fracture orientations: NW-SE, NE-SW and N-S trend.

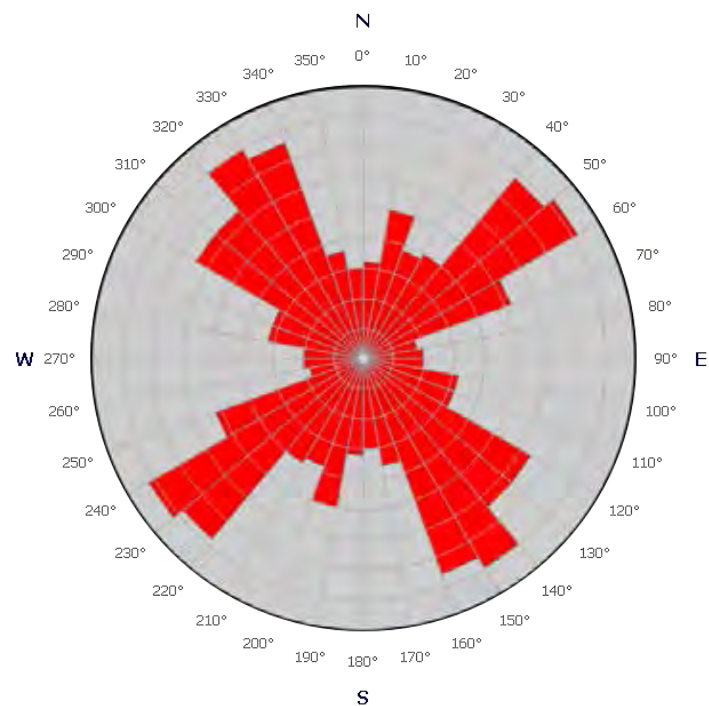


Figure 4.6 Rose diagram showing fracture strike orientation and frequency of Phasudpandin derived by Mesh selection Analysis. Showing three main fracture orientations: NNW-SSE, NE-SW and NNE-SSW.

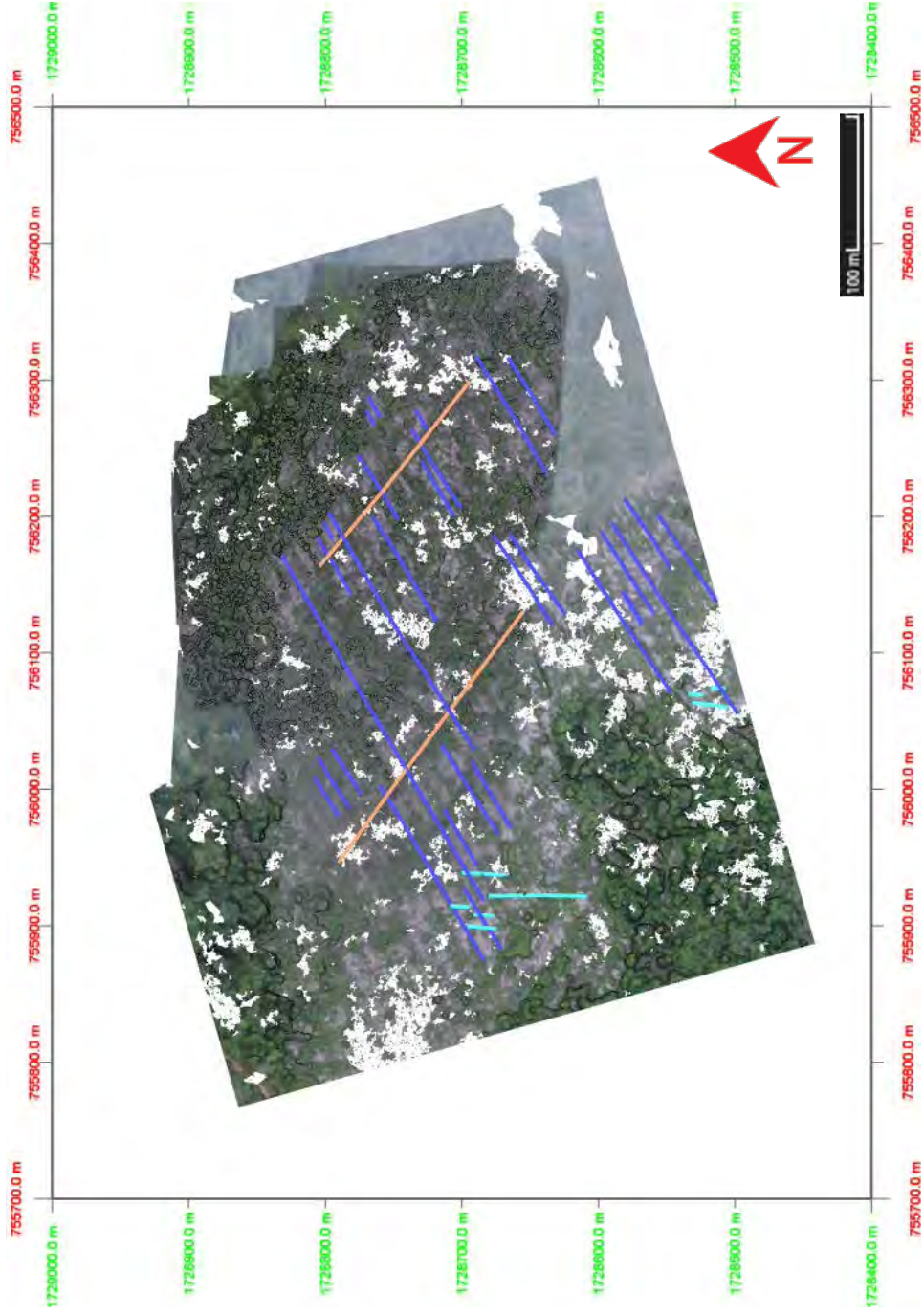


Figure 4.7 Digital outcrop model of Pahingam national park. Light blue, dark blue and orange lines representing N-S, NE-SW and NNW-SSE strike orientations of fracture respectively, are derived by visual interpretation.

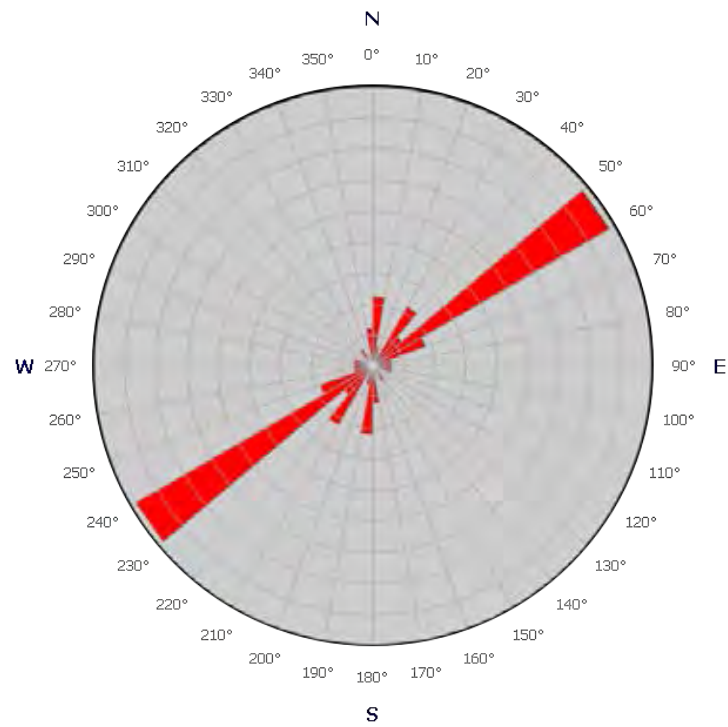


Figure 4.8 Rose diagram showing fracture strike orientation and frequency of Pahingam national park derived by visual interpretation. Showing two main fracture orientations: NE-SW and N-S.

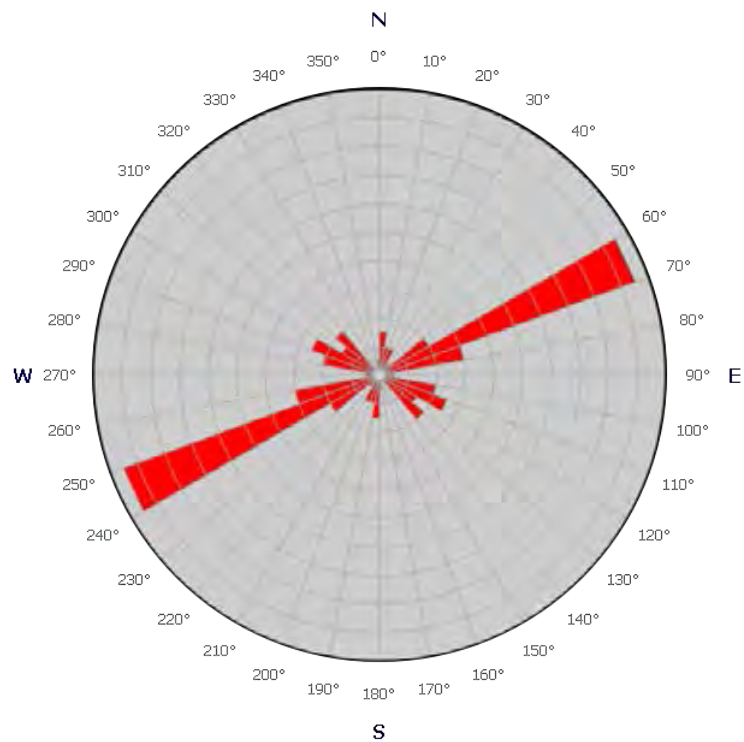


Figure 4.9 Rose diagram showing fracture strike orientation and frequency of Thep Phana waterfall in Thep sathit district. Showing three main fracture orientations: WNW-ESE, ENE-WSW and N-S.

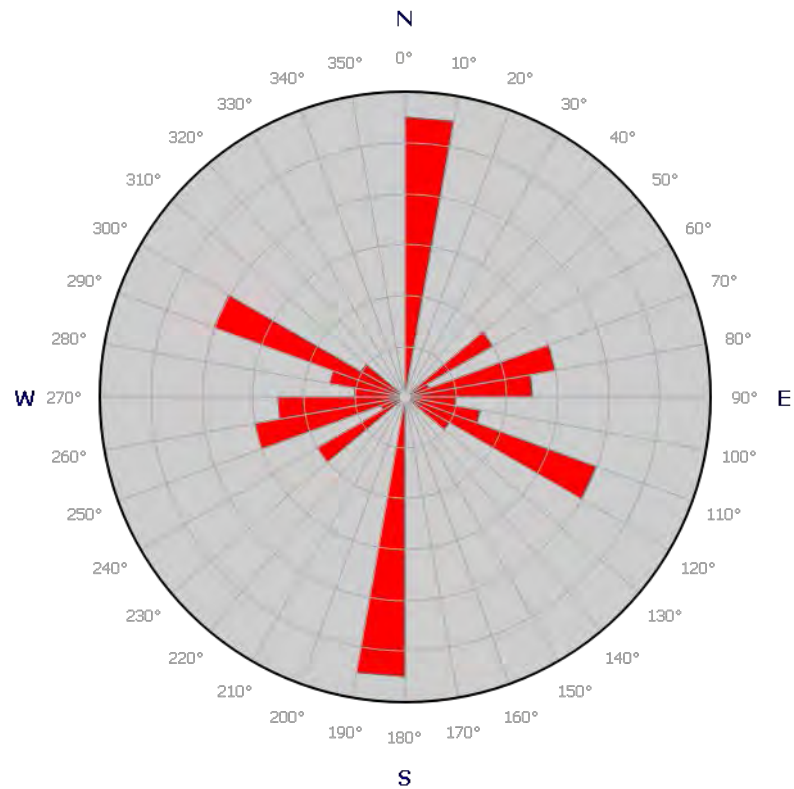


Figure 4.10 Rose diagram showing fracture strike orientation and frequency of Thep Prathan waterfall in Thep sathit district. Showing three main fracture orientations: WNW-ESE, ENE-WSW and N-S.

4.2 Fracture classification

From field survey data, there are 3 main strike orientations of fracture: WNW-ESE, ENE-WSW and N-S (Fig 4.11).

WNW-ESE trend is shear fracture. It is dextral strike-slip fracture indicated by slickensides and slickenlines along fracture plane (Fig 4.12, 4.13, 4.14). Its slickenlines lie in WNW-ESE direction ranging from 290 to 300 degrees with plunge between 0 and 10 degrees.

ENE-WSW trend is shear fracture. It is sinistral strike-slip fracture indicated by slickensides and slickenlines along fracture plane (Fig 4.15, 4.16, 4.17) and extensional bend (Fig 4.18, 4.19). Its slickenlines lie in ENE-WSW direction ranging from 60 to 70 degrees with plunge between 0 and 10 degrees.

N-S trend is extension fracture that shows relatively perpendicular displacement compared to the wall. However, there is no evidence for movement along the fracture plane (Fig 4.20, 4.21, 4.22).



Figure 4.11 Three directions of fracture in Thep Phana waterfall.



Figure 4.12 WNW-ESE trending dextral strike-slip fracture in Thep Phana waterfall showing slickensides along fracture plane.



Figure 4.13 WNW-ESE trending dextral strike-slip fracture in Thap Prathan waterfall showing slickensides along fracture plane.



Figure 4.14 WNW-ESE trending dextral strike-slip fracture in Wat Nam Tok Charoen Tham showing slickensides along fracture plane.



Figure 4.15 ENE-WSW trending sinistral strike-slip fracture in Thep Phana waterfall showing slickensides along fracture plane.



Figure 4.16 ENE-WSW trending sinistral strike-slip fracture in Phasudpandin showing slickensides along fracture plane.



Figure 4.17 ENE-WSW trending sinistral strike-slip fracture in Wat Nam Tok Charoen Tham showing slickensides along fracture plane.



Figure 4.18 ENE-WSW trending sinistral strike-slip fracture in Thep Phana waterfall showing slickensides along fracture plane.



Figure 4.19 ENE-WSW trending sinistral strike-slip fracture in Thep Prathan waterfall showing slickensides along fracture plane.



Figure 4.20 N-S trending open fracture in Thep Phana waterfall showing no evidence for movement along fracture plane.



Figure 4.21 N-S trending open fracture in Phasudpandin showing no evidence for movement along fracture plane.



Figure 4.22 N-S trending open fracture in Wat Nam Tok Charoen Tham showing no evidence for movement along fracture plane.

4.3 Stress Analysis

There are three consistent trends of fracture derived from Digital elevation model, Digital outcrop model, and Field observation which are WNW-ESE trend ranging from 290 to 310 degrees, ENE-WSW trend ranging from 50 to 80 degrees and N-S trend ranging from 340 to 10 degrees. From field observation, WNW-ESE, ENE-WSW and N-S trend are identified as dextral strike-slip fracture, sinistral strike-slip fracture and Extension fracture respectively. All fracture trends are subvertical, while slickenlines are subhorizontal, so maximum compressive principle stress (σ_1) is on horizontal plane. In this study, dihedral angle is about 125 degrees. Maximum compressive principle stress, analysed from this angle, lies in 2.5 degrees. Maximum compressive principle stress, analysed from stike of extension fracture, lies in 340 to 10 degrees. Both are consistent, so maximum compressive principle stress lies in the range of 340 to 10 degrees in horizontal plane (Fig 4.23).

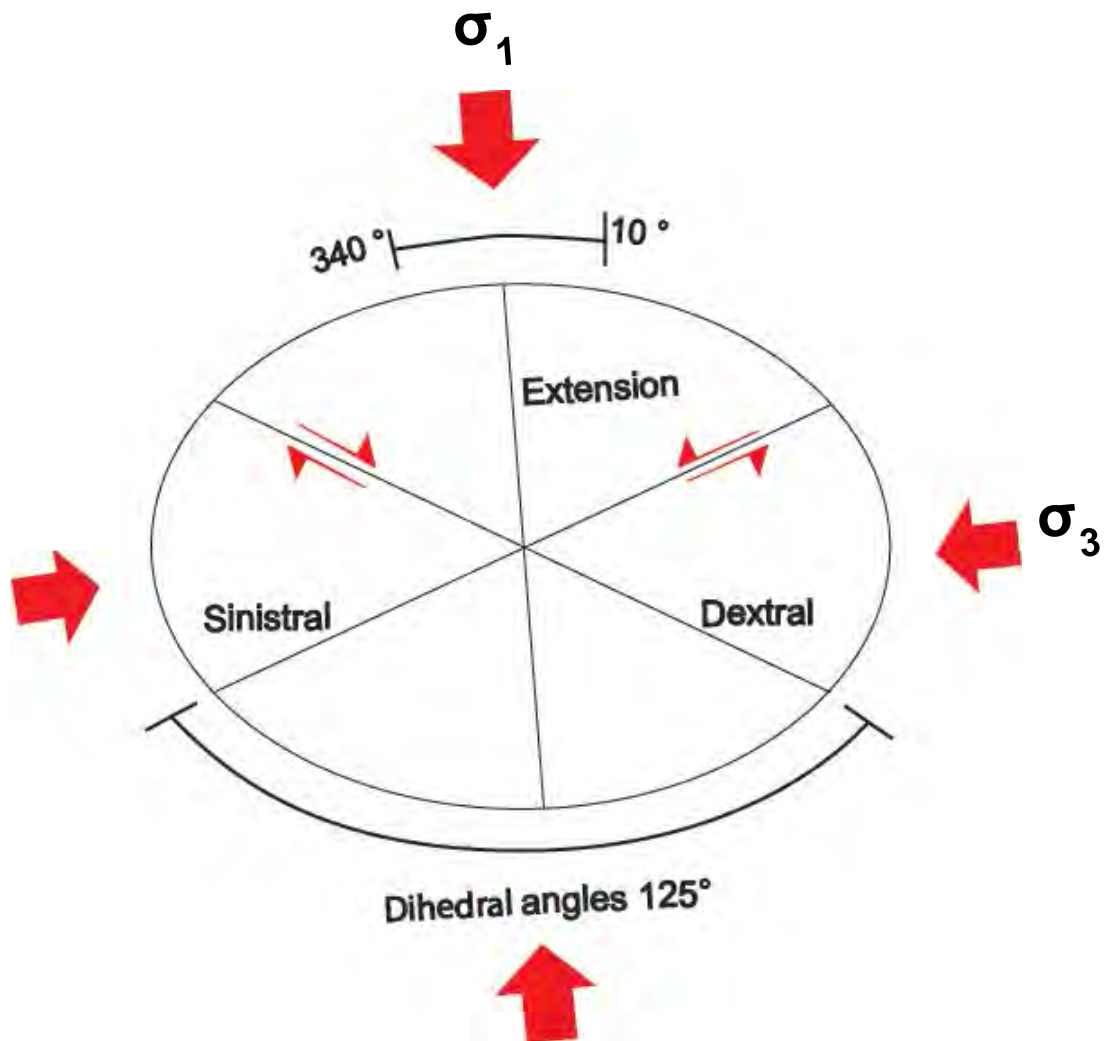


Figure 4.23 2D stress ellipse showing types and trends of fracture, the dihedral angle and range of σ_1 direction.

Chapter 5

Discussions

5.1 Mesh selection analysis and visual interpretation

Mesh selection analysis and visual interpretation provide similar fracture orientation but not the same (Fig 4.5,4.6). There are two reasons why both aren't the same. The first is one fracture plane consist of a lot of meshes and fracture plane isn't smooth surface, so one fracture has variation of mesh orientation (Fig 3.7). The second is one fracture plane is not counted as one frequency in mesh selection mean. Fracture length has influence to frequency of fracture trend. Long fracture has more meshes than short fracture, so frequency of the long fracture is greater than the short trend in rose diagram. While in visual interpretation, one fracture is counted as one frequency. Visual interpretation give more reliable result because fracture length shouldn't affect to frequency of fracture occurred in the same scale. In this study, results of fracture orientation, is used to analyze stress state, are results from visual interpretation.

5.2 E-W fracture trend in DEM

Figure 4.2 shows that there is fracture lying in E-W trend. This trend isn't consistent with fracture trends from field observation. This trend may be river channel. In Thep Sathit district, western area has high elevation than eastern area showed in digital elevation model (Fig 5.2), results water flow in E-W direction. The other assumption is this trend is Release fracture. When the stress acting on a rock is released, the rock relaxes to get a different shape. This change in shape can create tensile stress that are sufficient to release fracture.

5.3 Maximum compressive principle stress direction

Maximum principle stress direction is obtained by 2 means: Bisectors of conjugate shear fracture and orientation of extension fracture. Maximum principle stress direction based on the acute bisectors of conjugate shear fracture may not be accurate if dihedral angle are unusually large (Ismat, 2015). Therefore, maximum principle stress direction in this study mainly base on the orientation of extension fracture.

5.4 Unusual high dihedral angle

Dihedral angle of shear fracture in this study is about 125 degrees. This dihedral angle is inconsistent with Mohr-Coulomb theory. From field observation, there is no evidence for pressure solution, e.g. stylolite, in this area. Therefore, the high dihedral

angle is resulted from fracturing occurred when rock was in deep in crust or within the fold's hinge region.

5.5 Conceptual model for fracture development

According to stress state result in chapter 4, N-S compression in the cause of fracturing in the western part of Thep Sathit district. This study focuses only on fractures in Phra Wihan formation, the formation that deposited in Early Cretaceous. Tectonic event which caused the fracturing must be the event occurred after Early Cretaceous. There are two events after Early Cretaceous: Mid-Cretaceous event and Himalayan Orogeny event (Fig 2.2). Mid-Cretaceous event, caused by the collision between West Burma plate and Sibumasu plate (Gardiner et al., 2016), resulted in E-W compression, so this event doesn't relate to fracturing in western part of Thep Sathit district. Himalayan Orogeny caused by the collision between India plate and Eurasia plate in Middle Eocene (Morley, 2012), resulted in N-S compression in South East Asia. Therefore, this tectonic event is the cause of fracturing in study area.

Fracture often form as subsidiary features and are related to other structures such as fracture associated with fold, fracture associated with fault. According to tranpression, folding, thrusting and erosion of Khorat Group that occurred in Middle Miocene (Searle & Morley, 2011), and Apatite fission track found in the study area which indicates the uplifting of western margin of Khorat plateau in Middle Eocene (41 ± 4) (Upton, 1999), fracture along western margin of Thep Sathit district possibly occurred simultaneously with the lifting of Khorat plateau.

Lifting of the cliff was controlled by fault, so fault along western margin of Thep Sathit district simultaneously with the fracturing in western part of Thep Sathit district. N-S compression, which was cause of fracturing, suggest that the fault is sinistral strike-slip fault. This fault consistent with sinistral strike-slip fault from Morley (2012) (Fig 5.3).

Digital elevation model shows western area of district has high elevation than nearby area. Rising up of this area is controlled by reverse fault related with tranpression which resulted from sinistral strike-slip fault (Fig 5.3,5.4). This assumption is supported by high dihedral angle. The high dihedral angle indicates that the fractured rock used to be in deeper crust or within fold's hinge region before.

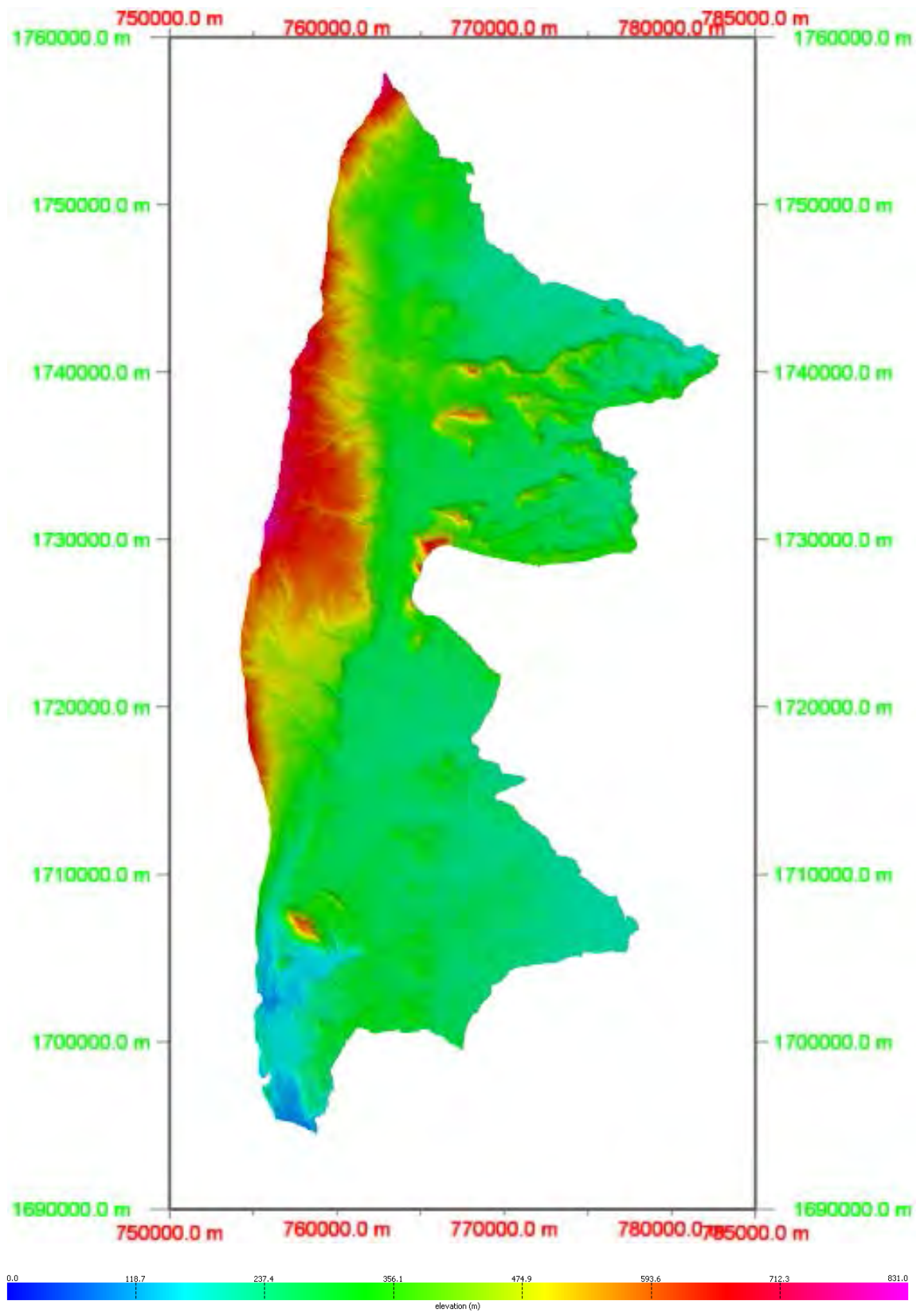


Figure 5.1 Digital elevation model of Thep Sathit showing wester area has high elevation than eastern area.

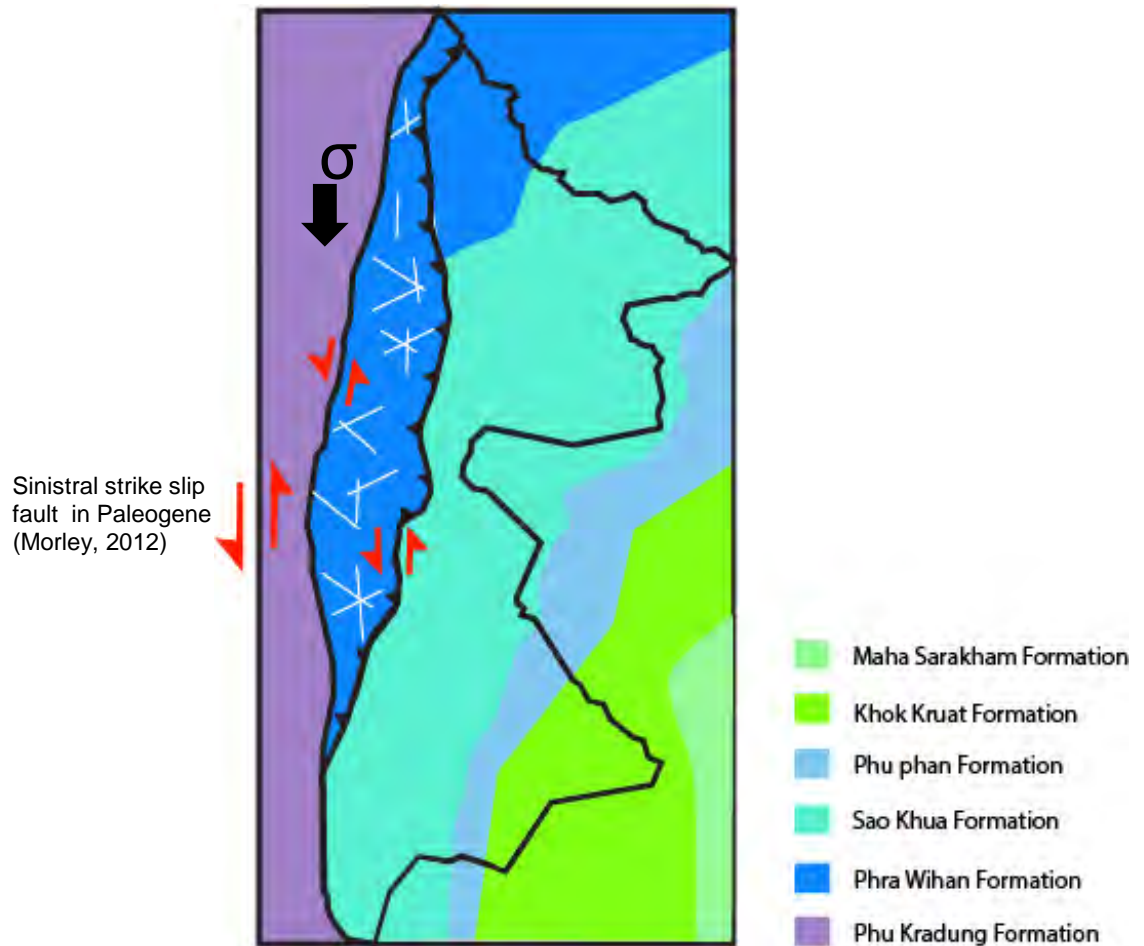


Figure 5.2 Sinistral strike-slip fault along western margin of Khorat plateau and reverse fault in western area of district are resulted from N-S compression.

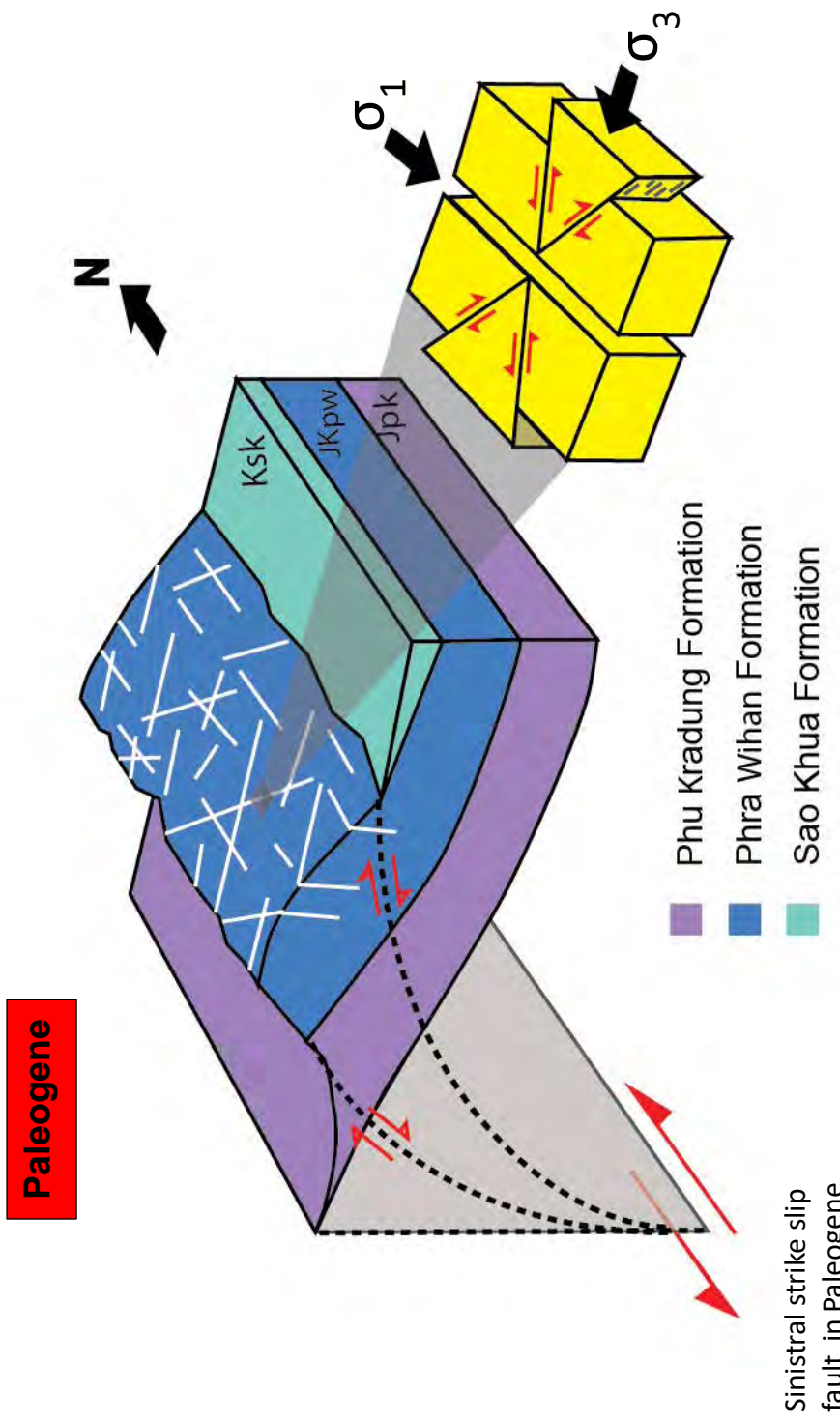


Figure 5.3 Conceptual model for fracture development showing fracture, high elevation area in western part of Thep Sathit district and sinistral strike-slip fault are resulted from N-S compression in Paleogene.

Chapter 6

Conclusion

This study considered data from field observation, digital outcrop model and digital elevation model to create fracture map and conceptual model for fracture development. Result, which are showed in rose diagram and stress ellipse, and discussion about conceptual model for fracture development can be summarized from these following.

- Fractures in this study area mainly lie in WNW-ESE (290°-310°), ENE-WSW (50°-80°) and N-S(340°-10°) trending.
- All trends of fracture are sub-vertical fracture plane.
- WNW-ESE is dextral strike-slip fracture and has slickenlines which lie in WNW-ESE (290°-300°) with horizontal plunge (0°-10°). ENE-WSW is sinistral strike-slip fracture and has slickenlines which lie in ENE-WSW(60°-70°) with horizontal plunge (0 -10°). N-S trend is extension fracture.
- Stress analysis from fracture orientation and type of fracture indicates that there is one event of deformation. Maximum compressive principle stress lies in N-S direction (340°-10°) in horizontal plane.
- N-S compression was caused by collision of India plate and Eurasia plate in Paleogene. This compression resulted in lifting and faulting of western margin of Thep Sathit. Moreover, this comperssion direction suggest that fault along western margin of Thep Sathit is sinistral stike-slip fault.

References

- Booth, J. E. 1998. The Khorat Plateau of NE Thailand exploration history and hydrocarbon potential. SEAPEX Exploration Conference, Singapore, 169–203.
- Booth, J. and Sattayarak, N. 2011. Subsurface Carboniferous-Cretaceous geology of NE Thailand. In: Ridd, M.F. Barber, A.J. and Crow, M.J. (eds), *The Geology of Thailand*, The Geological Society of London, pp. 185-222.
- Cooper, M. A., Herbert, R. & Hill, G. S. 1989. The structural evolution of Triassic intermontane basins in Northeast Thailand. In: Thanasuthipitak, T. & Ounchanum, P. (eds) *Proceedings of the International Symposium on Intermontane Basins: Geology and Resources*. Chiang Mai University, Chiang Mai, 231–242.
- Department of Mineral Resources. 2007. Geologic map of Thailand 1:1000000, Geological survey Division, Department of Mineral Resources, Bangkok, Thailand
- Gardiner, N.J., Robb, L.J., Morley, C.K., Searle, M.P., Cawood, P.A., Whitehouse, M.J., Kirkland, C.L., Roberts, N.M. and Myint, T.A., 2016. The tectonic and metallogenic framework of Myanmar: a Tethyan mineral system. *Ore Geology Reviews*, 79, pp.26-45.
- Ismat, Z., 2015. What can the dihedral angle of conjugate-faults tell us?. *Journal of Structural Geology*, 73, pp.97-113.
- Jirapat, P., 2016. Structural geology of Carbonate rocks in Siam City Cement Public Company Limited, Amphoe Kaeng Khoi, Changwat Saraburi. Unpublished senior project, Chulalongkorn University, 44pp.
- Lovatt-Smith, P. F., Stokes, R. B., Bristow, C. & Carter, A. 1996. Mid-Cretaceous inversion in the Northern Khorat Plateau of Lao PDR and Thailand. In: Hall, R. & Blundell, D. (eds) *Tectonic Evolution of Southeast Asia*. Geological Society, London, Special Publications, 106, 97–122.
- Masoud, A. and Koike, K., 2017. Applicability of computer-aided comprehensive tool (LINDA: LINEament Detection and Analysis) and shaded digital elevation model for characterizing and interpreting morphotectonic features from lineaments. *Computers & Geosciences*, 106, pp.89-100.
- Meesook, A. 2011. Cretaceous. In: Ridd, M.F., Barber, A.J. & Crow, M.J. (eds) *The Geology of Thailand*. Geological Society, London, 170-184.
- Metcalf, I. 1996. Pre-Cretaceous evolution of SE Asian terranes. In: Hall, R. & Blundell, D. (eds) *Tectonic Evolution of Southeast Asia*. Geological Society, London, Special Publications, 106, 97–122.
- Morley, C.K., 2012. Late Cretaceous–early Palaeogene tectonic development of SE Asia. *Earth-Science Reviews*, 115(1-2), pp.37-75
- Peacock, D.C.P. and Sanderson, D.J., 1995. Pull-aparts, shear fractures and pressure solution. *Tectonophysics*, 241(1-2), pp.1-13.

- Racey, A., 2009. Mesozoic red bed sequences from SE Asia and the significance of the Khorat Group of NE Thailand. Geological Society, London, Special Publications, 315(1), pp.41-67.
- Racey, A. and Goodall, J.G., 2009. Palynology and stratigraphy of the Mesozoic Khorat Group red bed sequences from Thailand. Geological Society, London, Special Publications, 315(1), pp.69-83.
- Searle, M.P. and Morley, C.K., 2011. 20 Tectonic and thermal evolution of Thailand in the regional context of SE Asia.
- Upton, D. R. 1999. A Regional Fission Track Study of Thailand: Implications for Thermal History and Denudation. Unpublished PhD thesis University of London, 158pp.
- Warren, J., Morley, C. K., Charoentitirat, T., Cartwright, I., Ampaiwan, P., Khositichaisri, P., Mirzaloo, M., and Yingyuen, J. 2014. Structural and Fluid Evolution of Saraburi Group Sedimentary Carbonates, Central Thailand: A Tectonically Driven Fluid System. *Marine and Petroleum Geology* 55: pp. 100-121.

Appendix

St1	strike	dip	St1	strike	dip	St1	strike	dip
NW-SE trend	295	na	NW-SE trend	319	81	NE-SW trend	65	na
	283	na		310	68		61	na
	290	na		310	76		60	na
	297	na		313	74		60	na
	295	na		300	72		70	na
	288	na		300	85		65	na
	285	na		306	67		60	na
	285	na		strike	dip		65	na
	279	na		65	90		60	na
	294	na		65	na		70	na
St1	strike	dip	St1	strike	dip	St1	strike	dip
NE-SW trend	60	na	NE-SW trend	67	83	N-S trend	63	81
	65	na		62	na		65	83
	75	83		67	84		66	83
	81	83		51	84		60	89
	75	80		54	83		strike	dip
	73	83		61	86		183	na
	72	84		63	80		180	na
	60	79		62	78		194	80
	58	87		57	81		180	na
	60	81		67	83		175	na

Appendix 1 Fracture orientation which has collected from Thep Phana waterfall

St2	strike	dip	St2	strike	dip	St2	strike	dip	St2	strike	dip
NW-SE trend	292	na	NW-SE trend	278	81	NE-SW trend	70	88	NE-SW trend	70	88
	290	na		290	80		70	88			
	283	na		298	82		58	89			
	290	na	strike	dip	83		76				
	294	na	65	na	83		76				
NW-SE trend	304	na	NE-SW trend	57	na	N-S trend	83	76	N-S trend	80	80
	297	na		55	na		strike	dip			
	278	84		59	na		180	na			
	282	81		83	87		186	na			
	305	83		70	88		186	na			
St2	strike	dip	St2	strike	dip	St2	strike	dip	St2	strike	dip
N-S trend	187	na	N-S trend	187	na	N-S trend	187	na	N-S trend	187	na
	185	na		185	na		185	na			
	183	81		183	81		183	81			
	188	88		188	88		188	88			
	188	88		188	88		188	88			
	188	88		188	88		188	88			
	181	77		181	77		181	77			
	182	80		182	80		182	80			

Appendix 2 Fracture orientation which has collected from Thep Prathan waterfall

